Effects of shallow slope on the evolution of numerically simulated nocturnal low-level jets

Evgeni Fedorovich, Jeremy Gibbs, and Alan Shapiro

University of Oklahoma and *University of Utah*

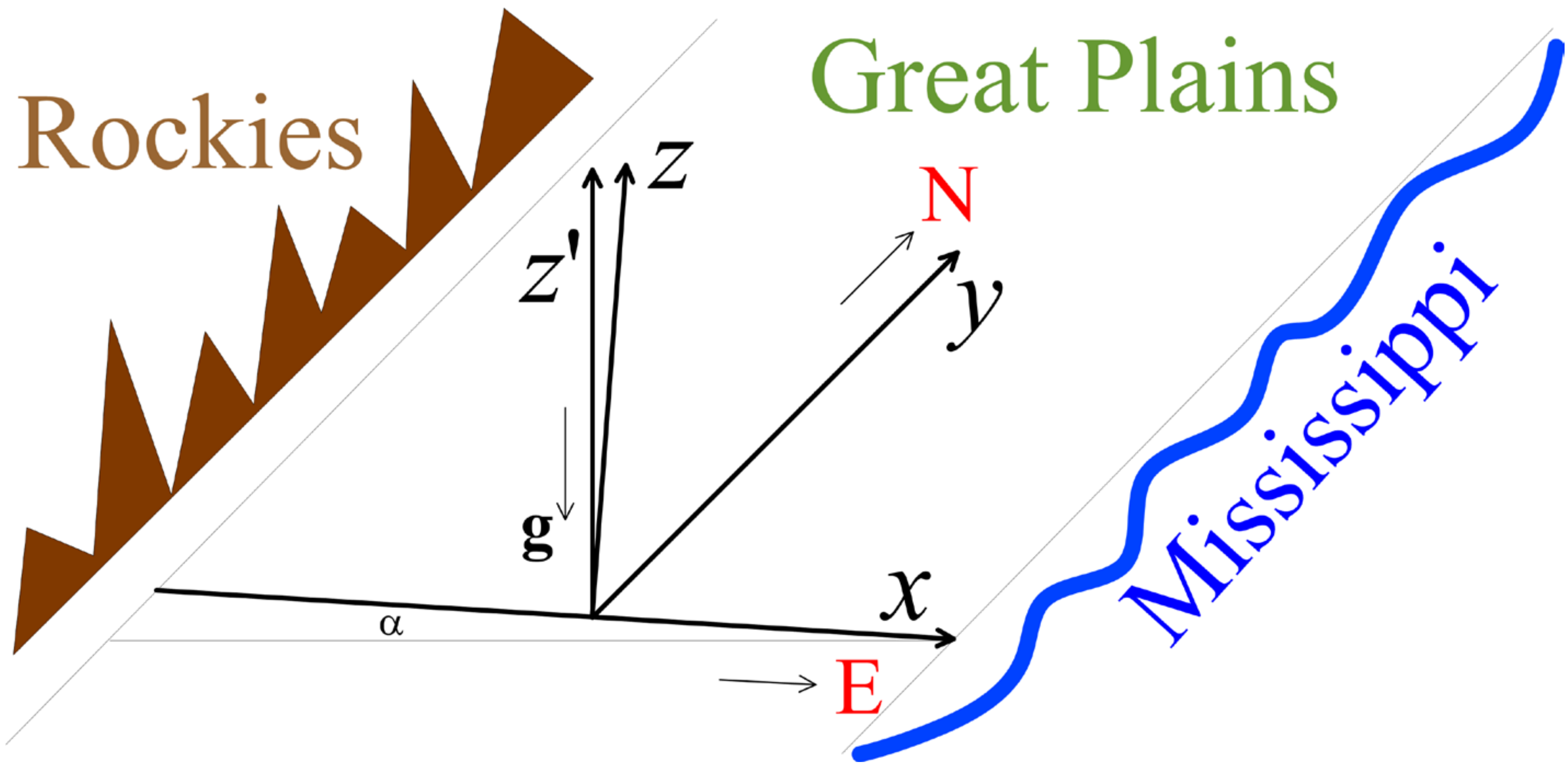

Terrain of the U.S. Great Plains

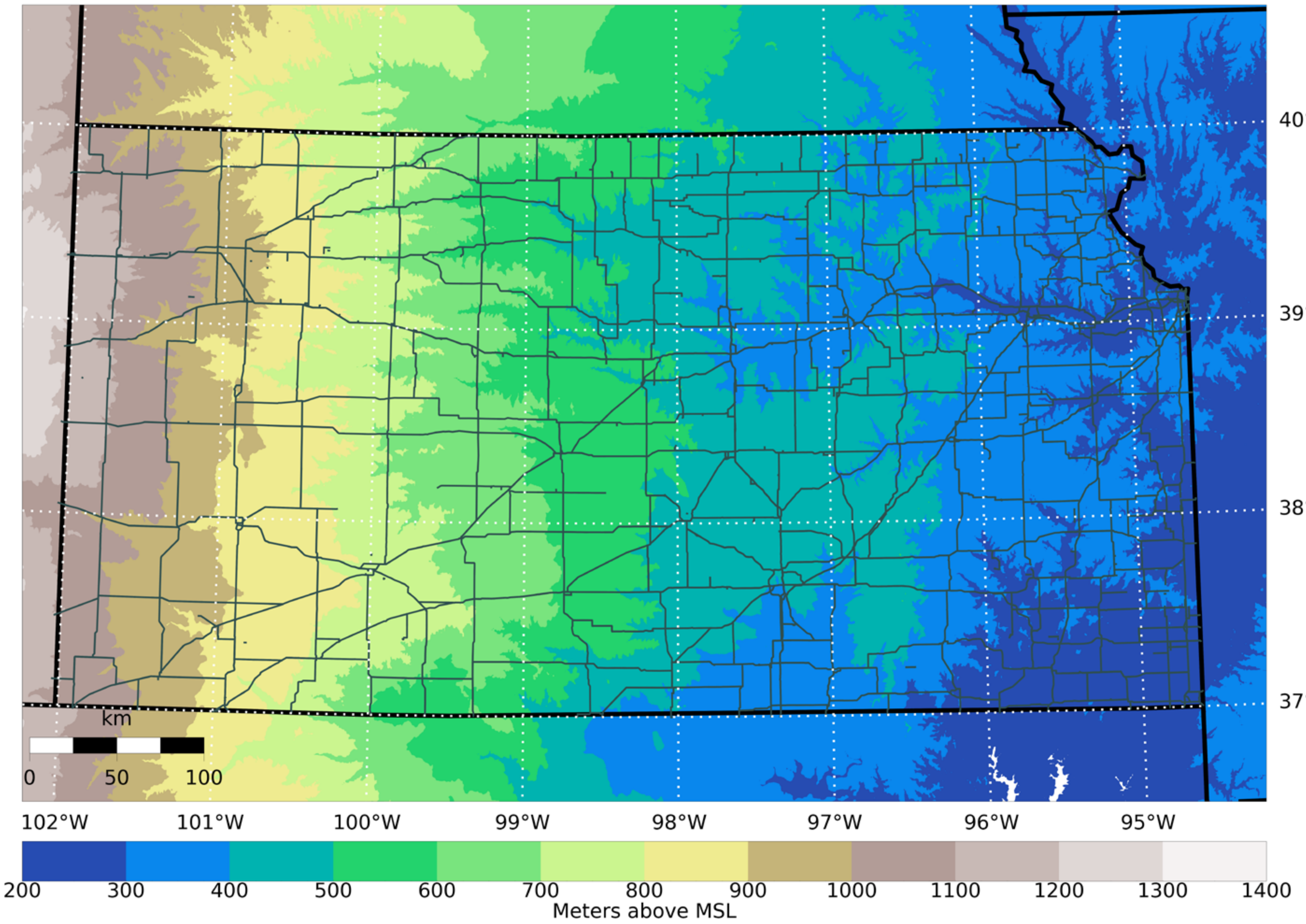

Nocturnal low-level jets over U.S. Great Plains

(examples from Klein et al. *BLM* 2016)

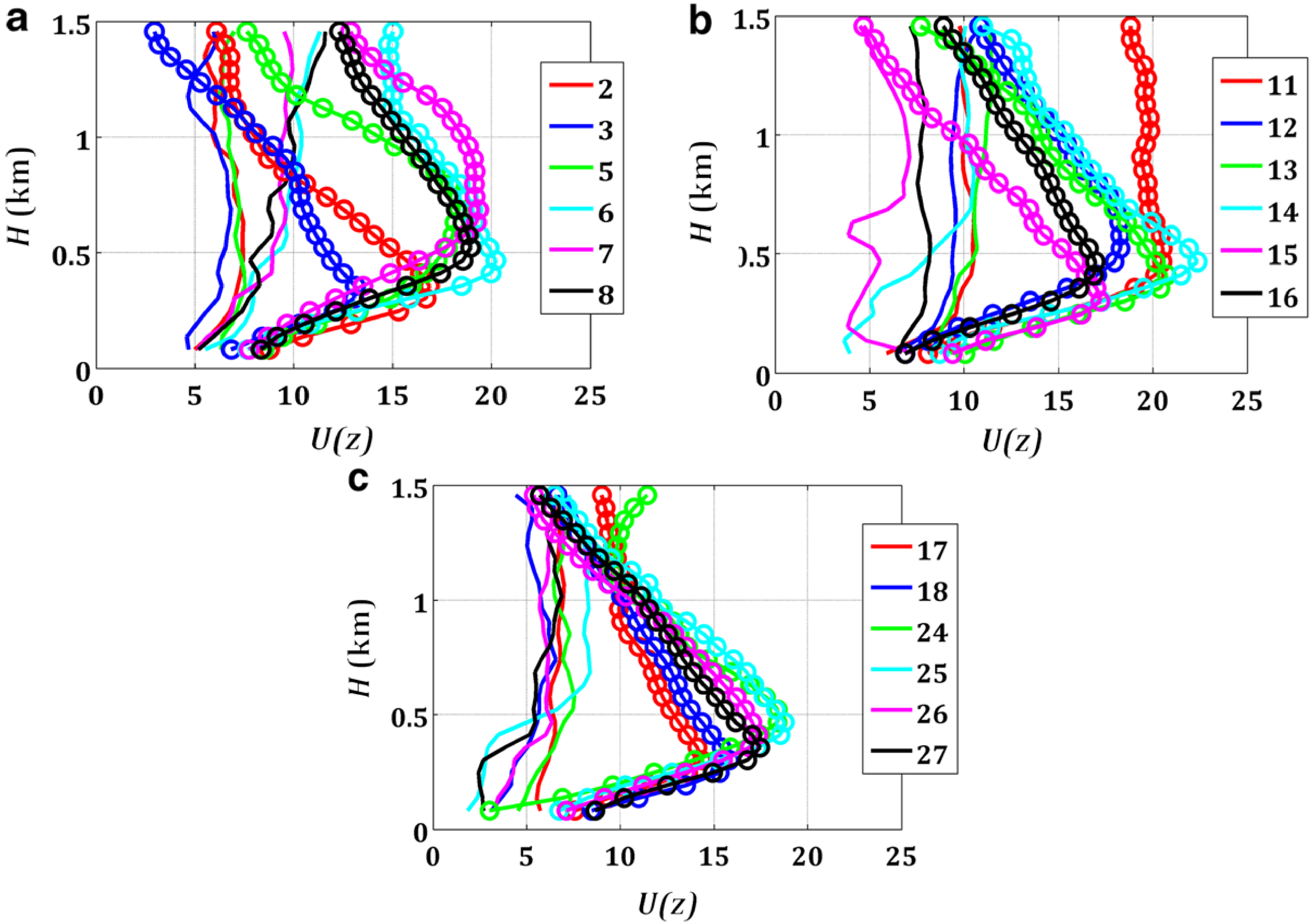

Flow variables in slope-following coordinates

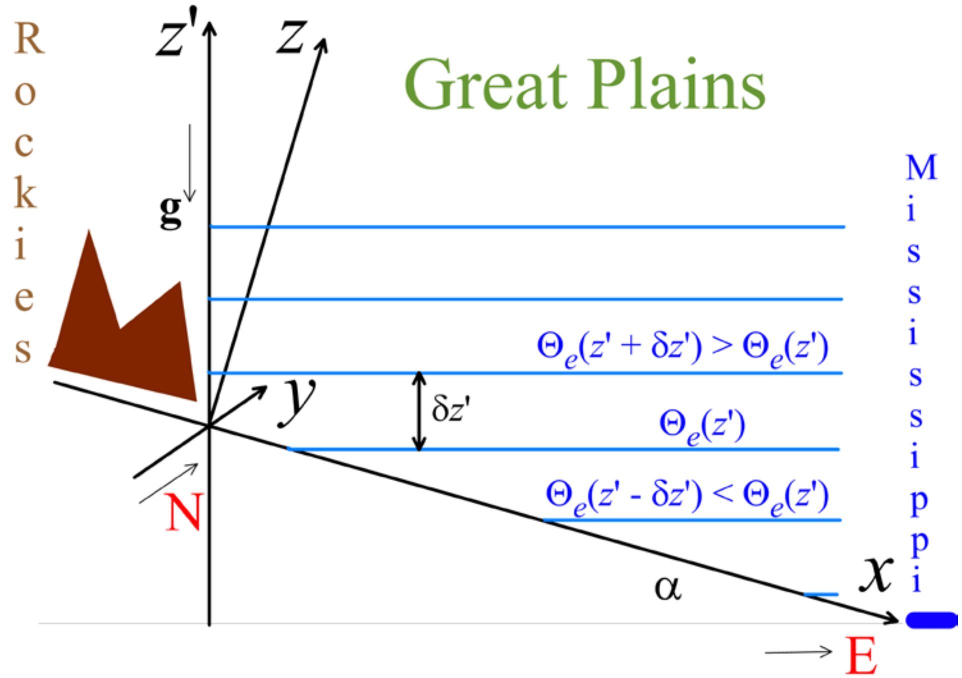

$u,\ v,\ w$ – velocity components along slope-following coordinates $x,\ y,\ z$;

$b = g[\Theta - \Theta_e(z')]/\Theta_r$ – buoyancy; $\Theta_e(z')$ – environmental potential temperature;

$\pi = [p - p_e(z')]/\rho_r$ – normalized p; $\gamma = d\Theta_e / dz' > 0$ – prescribed Θ_e gradient;

$f > 0$ – Coriolis parameter, V_g – geostrophic wind (known and directed along y);

$N = (g\gamma / \Theta_r)^{1/2}$ – Brunt-Väisälä frequency; α – slope angle ($\sim \pi / 1000 = 0.18^\circ$);

ν – kinematic viscosity, ν_h – thermal diffusivity (we take $\nu_h = \nu$, so $\Pr = \nu / \nu_h$ is 1).

Governing equations for boundary-layer flow on a slope

Momentum balance in Boussinesq approximation:

$$\frac{\partial u}{\partial t}+u\frac{\partial u}{\partial x}+v\frac{\partial u}{\partial y}+w\frac{\partial u}{\partial z}=-\frac{\partial \pi}{\partial x}+f(v-V_{\mathrm{g}})-b\sin\alpha+\nu\left(\frac{\partial^2 u}{\partial x^2}+\frac{\partial^2 u}{\partial y^2}+\frac{\partial^2 u}{\partial z^2}\right), \quad (1)$$

$$\frac{\partial v}{\partial t}+u\frac{\partial v}{\partial x}+v\frac{\partial v}{\partial y}+w\frac{\partial v}{\partial z}=-\frac{\partial \pi}{\partial y}-fu+\nu\left(\frac{\partial^2 v}{\partial x^2}+\frac{\partial^2 v}{\partial y^2}+\frac{\partial^2 v}{\partial z^2}\right), \quad (2)$$

$$\frac{\partial w}{\partial t}+u\frac{\partial w}{\partial x}+v\frac{\partial w}{\partial y}+w\frac{\partial w}{\partial z}=-\frac{\partial \pi}{\partial z}+b\cos\alpha+\nu\left(\frac{\partial^2 w}{\partial x^2}+\frac{\partial^2 w}{\partial y^2}+\frac{\partial^2 w}{\partial z^2}\right), \quad (3)$$

Thermal energy (buoyancy balance):

$$\frac{\partial b}{\partial t}+u\frac{\partial b}{\partial x}+v\frac{\partial b}{\partial y}+w\frac{\partial b}{\partial z}=N^2(u\sin\alpha-w\cos\alpha)+\nu_h\left(\frac{\partial^2 b}{\partial x^2}+\frac{\partial^2 b}{\partial y^2}+\frac{\partial^2 b}{\partial z^2}\right), \quad (4)$$

Mass conservation (continuity):

$$\frac{\partial u}{\partial x}+\frac{\partial v}{\partial y}+\frac{\partial w}{\partial z}=0. \quad (5)$$

Simulation setup

Boundary conditions

Lateral (x-y) conditions for u, v, w, b, and π are periodic.

Upper conditions (large z): $\partial\varphi / \partial z = 0$, where $\varphi = (u, v, b)$; $w = 0$,

and $\partial\pi / \partial z$ from the third equation of motion (3).

Lower conditions ($z = 0$): no-slip/impermeability ($u = v = w = 0$),

$\partial\pi / \partial z$ from (3), and $b = b_{\mathrm{s}}(t)$ or $B = -\nu(\partial b / \partial z)\big|_{z=0} = B_{\mathrm{s}}(t)$.

Initial state

Stably stratified atmosphere in the geostrophic equilibrium with linear $\Theta_e(z')$ and zero b.

Surface buoyancy forcing

At $0 < t \le \Delta t_{\mathrm{d}}$: $b_{\mathrm{sd}} = const > 0$ or $B_{\mathrm{sd}} = const > 0$.

At $t > \Delta t_{\mathrm{d}}$: $b_{\mathrm{sn}} = const < b_{\mathrm{sd}}$ or $B_{\mathrm{sn}} = const < 0$.

Simulation domain and grid

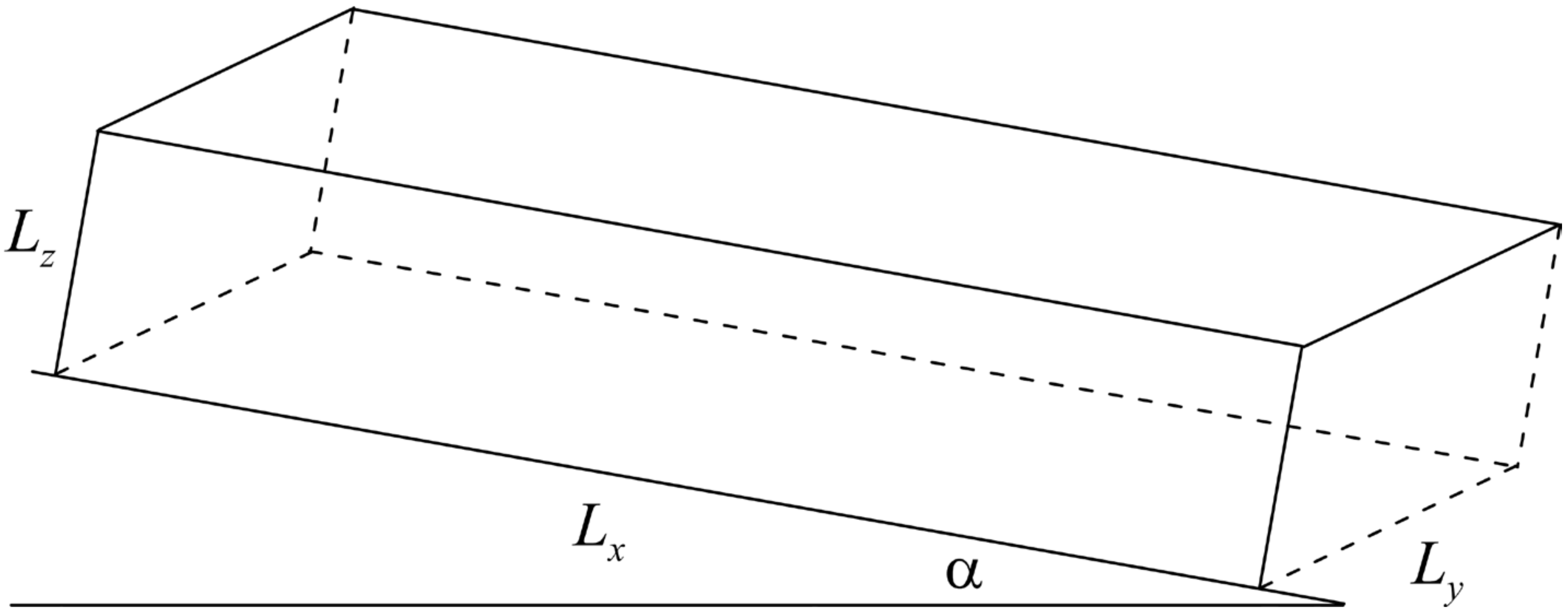

Dimensions (**L_i, rescaled to VAT) and grid node numbers N_i:**

$L_x, L_y = 1024 - 4096$ m; $N_x, N_y = 256 - 1024$; $L_z = 1536$ m, $N_z = 384$

Numerics: Micro HH (4³), developed by Chiel van Heerwaarden, with 4th order Runge-Kutta time integration, 4th order advection, and 4th order diffusion.

Slope-angle sensitivity of TKE and V: α = 0º, 0.09º, 0.18º, 0.27º

Surface buoyancy forcing case

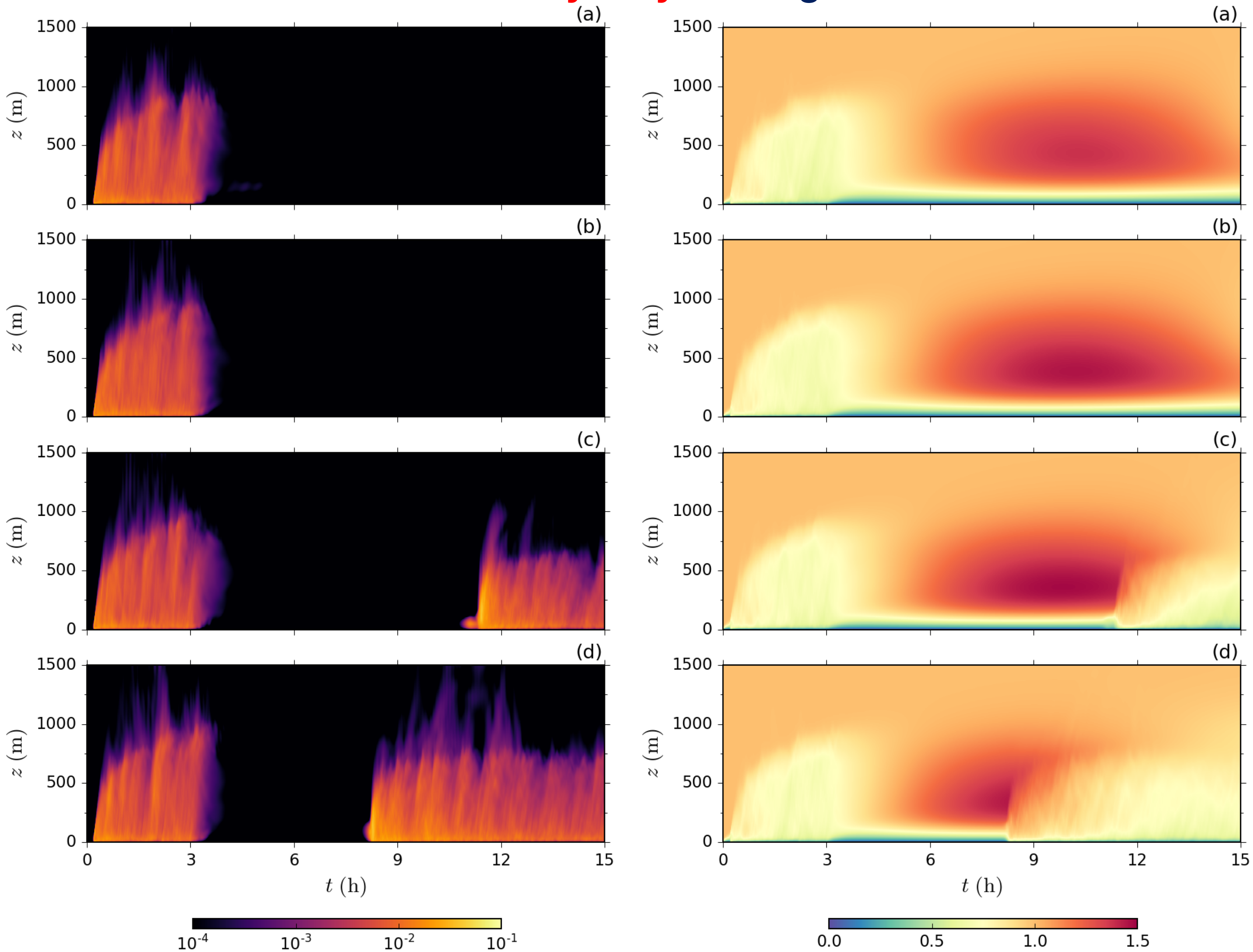

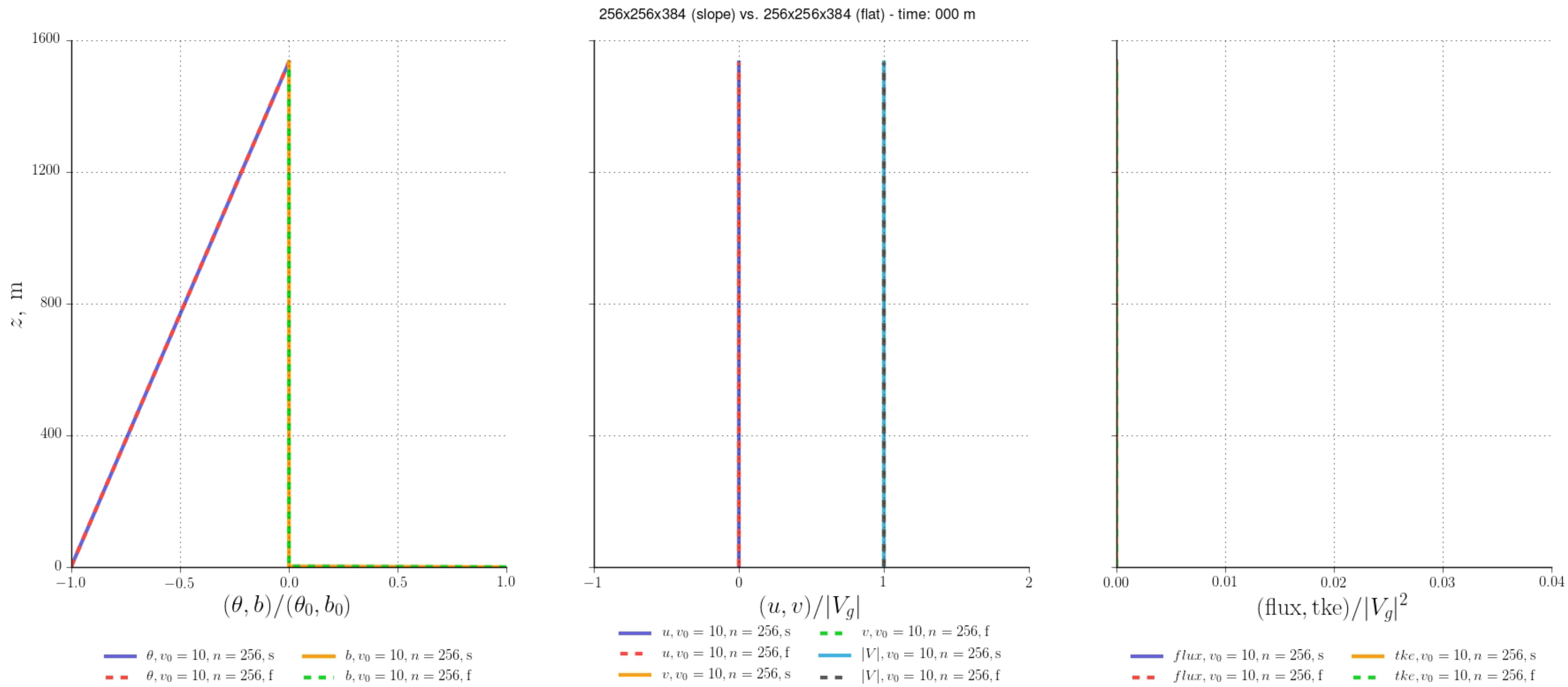

256x256x384 (slope) vs. 256x256x384 (flat) - time: 000 m
z, m
1600
1200
800
400
0
−1.0
−0.5
0.0
0.5
1.0
(θ, b)/(θ0, b0)
θ, v0 = 10, n = 256, s
θ, v0 = 10, n = 256, f
b, v0 = 10, n = 256, s
b, v0 = 10, n = 256, f
−1
0
1
2
(u, v)/|Vg|
u, v0 = 10, n = 256, s
u, v0 = 10, n = 256, f
v, v0 = 10, n = 256, s
v, v0 = 10, n = 256, f
|V|, v0 = 10, n = 256, s
|V|, v0 = 10, n = 256, f
0.00
0.01
0.02
0.03
0.04
(flux, tke)/|Vg|^2
flux, v0 = 10, n = 256, s
flux, v0 = 10, n = 256, f
tke, v0 = 10, n = 256, s
tke, v0 = 10, n = 256, f

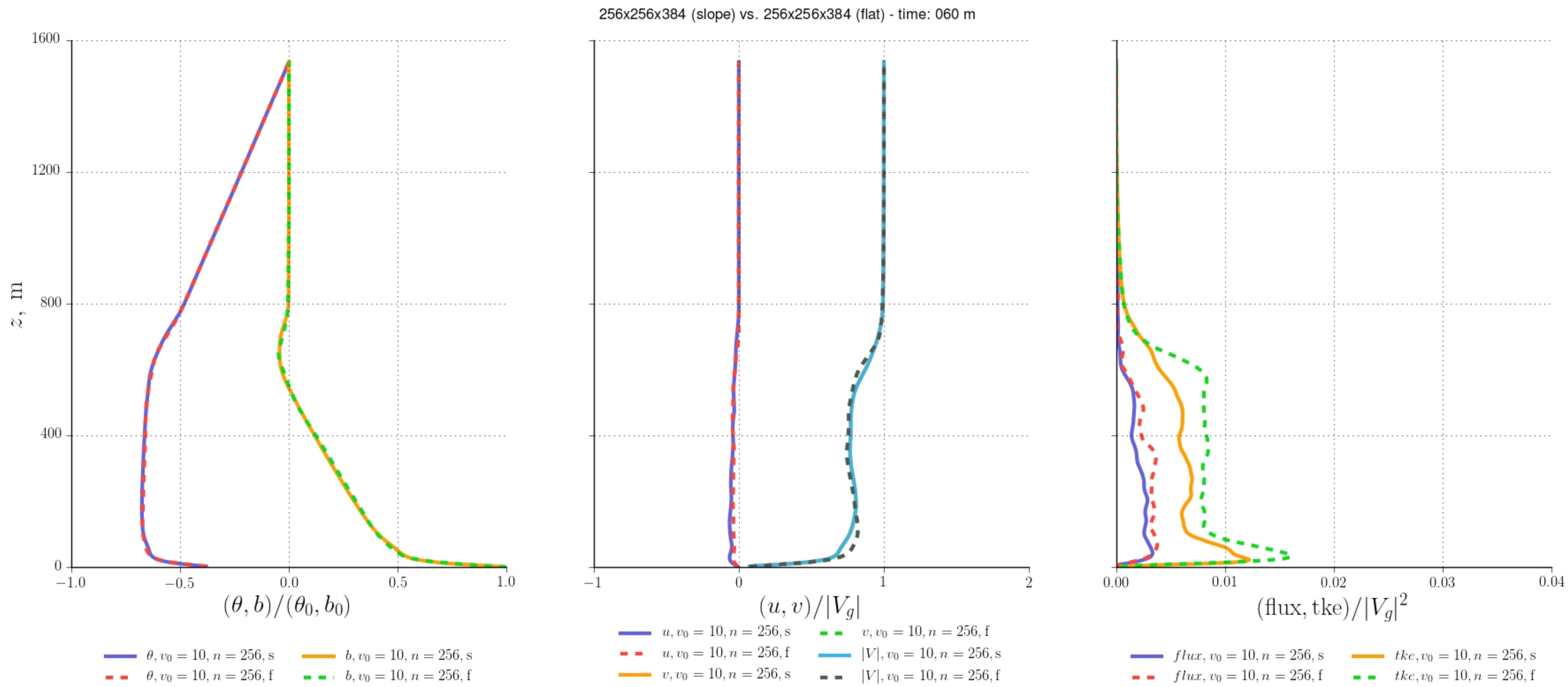

256x256x384 (slope) vs. 256x256x384 (flat) - time: 060 m
z, m
$(\theta, b)/(\theta_0, b_0)$
$(u, v)/|V_g|$
$(\mathrm{flux}, \mathrm{tke})/|V_g|^2$
$\theta, v_0 = 10, n = 256$, s
$\theta, v_0 = 10, n = 256$, f
$b, v_0 = 10, n = 256$, s
$b, v_0 = 10, n = 256$, f
$u, v_0 = 10, n = 256$, s
$u, v_0 = 10, n = 256$, f
$v, v_0 = 10, n = 256$, s
$v, v_0 = 10, n = 256$, f
$|V|, v_0 = 10, n = 256$, s
$|V|, v_0 = 10, n = 256$, f
$flux, v_0 = 10, n = 256$, s
$flux, v_0 = 10, n = 256$, f
$tke, v_0 = 10, n = 256$, s
$tke, v_0 = 10, n = 256$, f

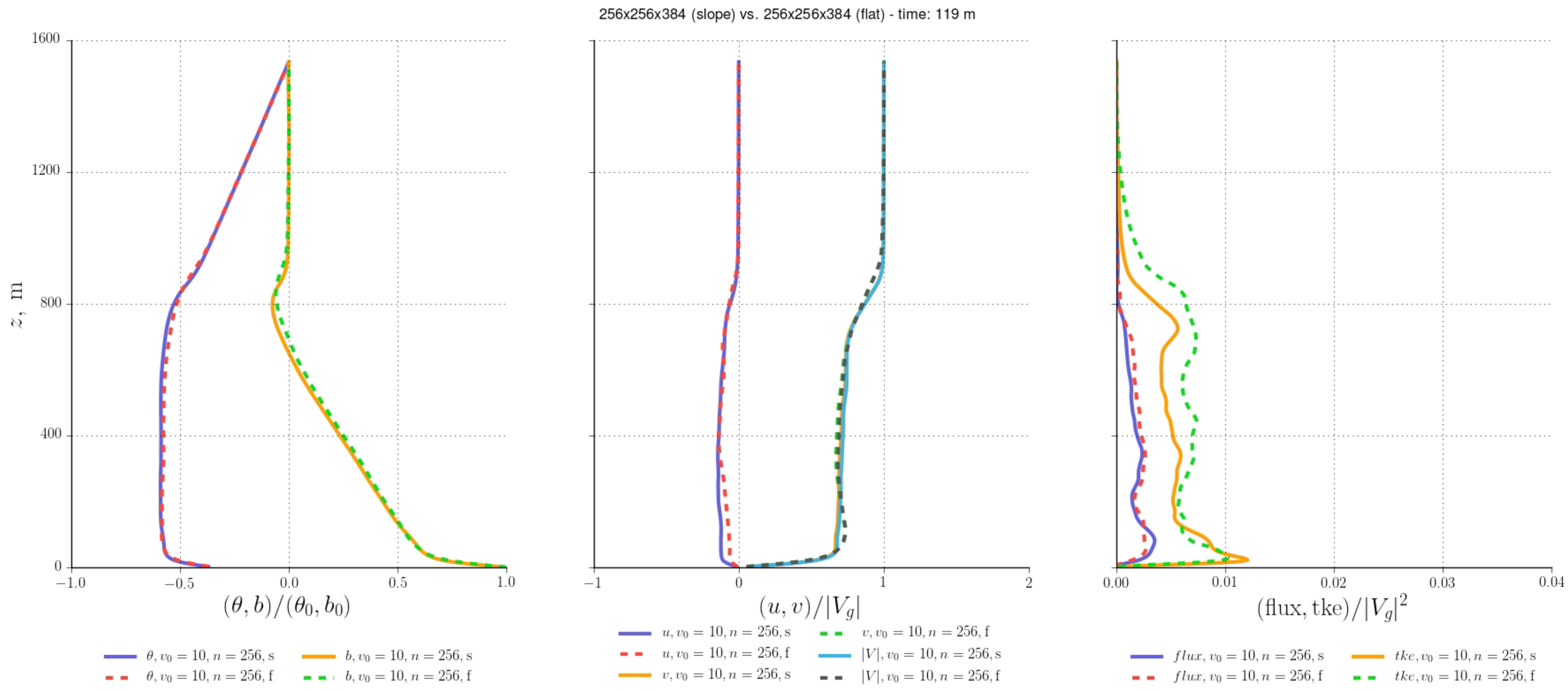
256x256x384 (slope) vs. 256x256x384 (flat) - time: 119 m
z, m
$(\theta, b)/(\theta_0, b_0)$
$(u, v)/|V_g|$
$(\mathrm{flux}, \mathrm{tke})/|V_g|^2$
$\theta, v_0 = 10, n = 256$, s
$\theta, v_0 = 10, n = 256$, f
$b, v_0 = 10, n = 256$, s
$b, v_0 = 10, n = 256$, f
$u, v_0 = 10, n = 256$, s
$u, v_0 = 10, n = 256$, f
$v, v_0 = 10, n = 256$, s
$v, v_0 = 10, n = 256$, f
$|V|, v_0 = 10, n = 256$, s
$|V|, v_0 = 10, n = 256$, f
$flux, v_0 = 10, n = 256$, s
$flux, v_0 = 10, n = 256$, f
$tke, v_0 = 10, n = 256$, s
$tke, v_0 = 10, n = 256$, f

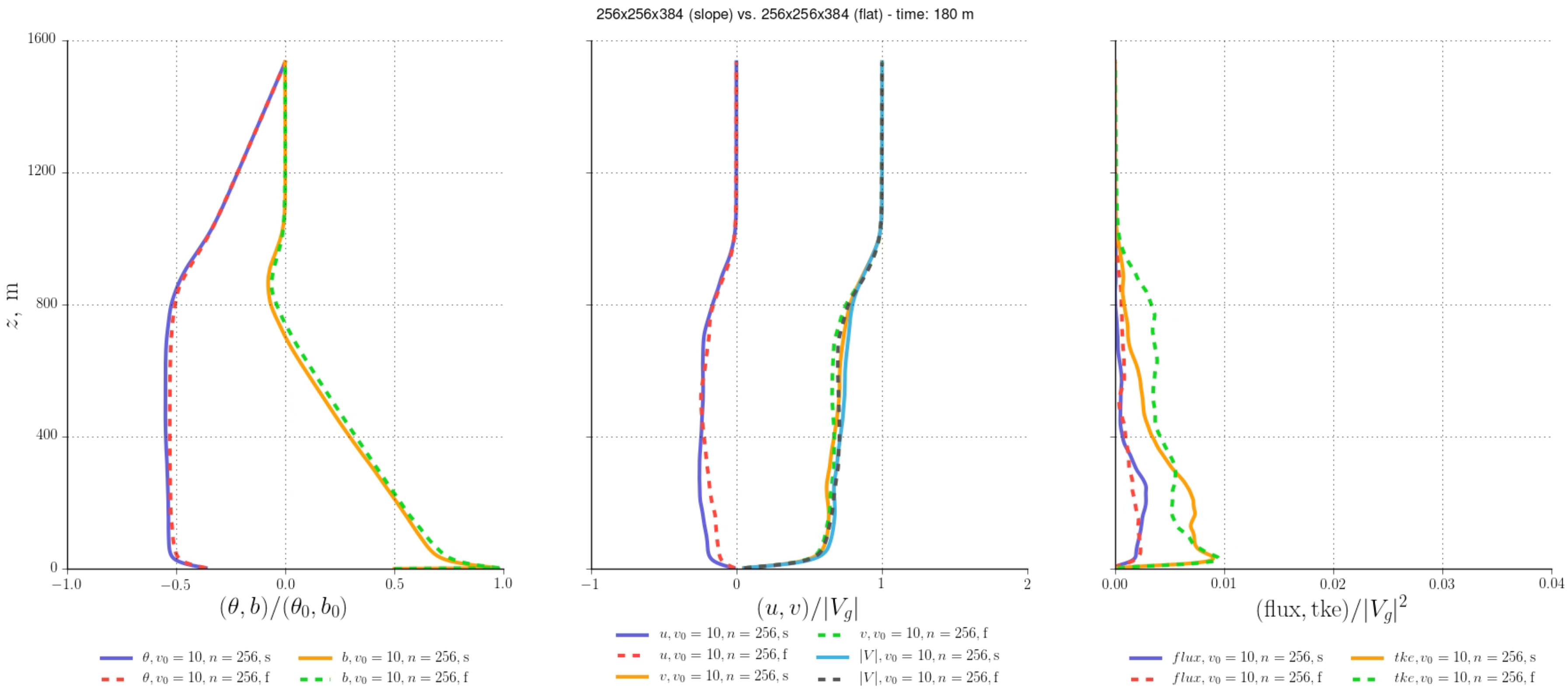
256x256x384 (slope) vs. 256x256x384 (flat) - time: 180 m
z, m
1600
1200
800
400
0
−1.0
−0.5
0.0
0.5
1.0
$(\theta, b)/(\theta_0, b_0)$
$\theta, v_0 = 10, n = 256$, s
$\theta, v_0 = 10, n = 256$, f
$b, v_0 = 10, n = 256$, s
$b, v_0 = 10, n = 256$, f
−1
0
1
2
$(u, v)/|V_g|$
$u, v_0 = 10, n = 256$, s
$u, v_0 = 10, n = 256$, f
$v, v_0 = 10, n = 256$, s
$v, v_0 = 10, n = 256$, f
$|V|, v_0 = 10, n = 256$, s
$|V|, v_0 = 10, n = 256$, f
0.00
0.01
0.02
0.03
0.04
$(\text{flux}, \text{tke})/|V_g|^2$
$flux, v_0 = 10, n = 256$, s
$flux, v_0 = 10, n = 256$, f
$tke, v_0 = 10, n = 256$, s
$tke, v_0 = 10, n = 256$, f

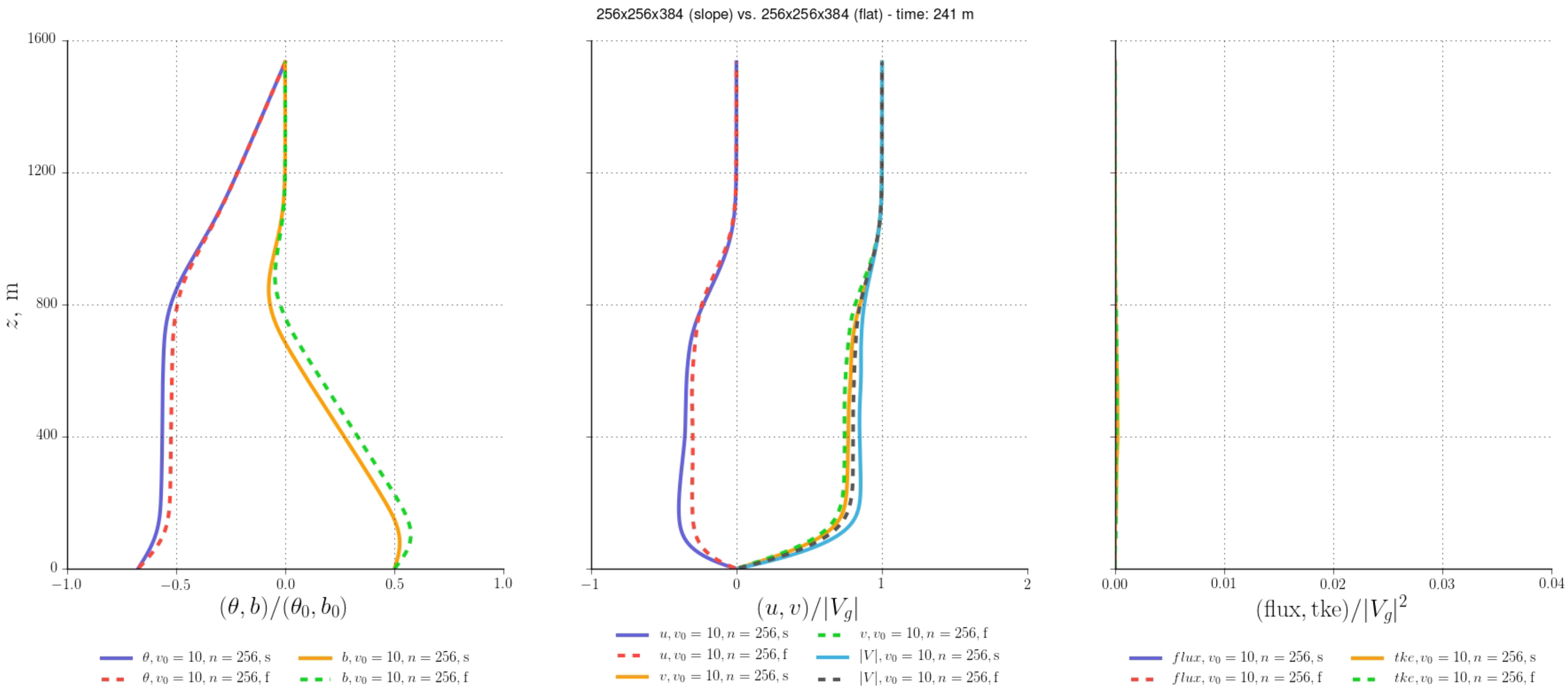
256x256x384 (slope) vs. 256x256x384 (flat) - time: 241 m
z, m
1600
1200
800
400
0
−1.0
−0.5
0.0
0.5
1.0
$(\theta, b)/(\theta_0, b_0)$
$\theta, v_0 = 10, n = 256$, s
$\theta, v_0 = 10, n = 256$, f
$b, v_0 = 10, n = 256$, s
$b, v_0 = 10, n = 256$, f
−1
0
1
2
$(u, v)/|V_g|$
$u, v_0 = 10, n = 256$, s
$u, v_0 = 10, n = 256$, f
$v, v_0 = 10, n = 256$, s
$v, v_0 = 10, n = 256$, f
$|V|, v_0 = 10, n = 256$, s
$|V|, v_0 = 10, n = 256$, f
0.00
0.01
0.02
0.03
0.04
$(\mathrm{flux}, \mathrm{tke})/|V_g|^2$
$flux, v_0 = 10, n = 256$, s
$flux, v_0 = 10, n = 256$, f
$tke, v_0 = 10, n = 256$, s
$tke, v_0 = 10, n = 256$, f

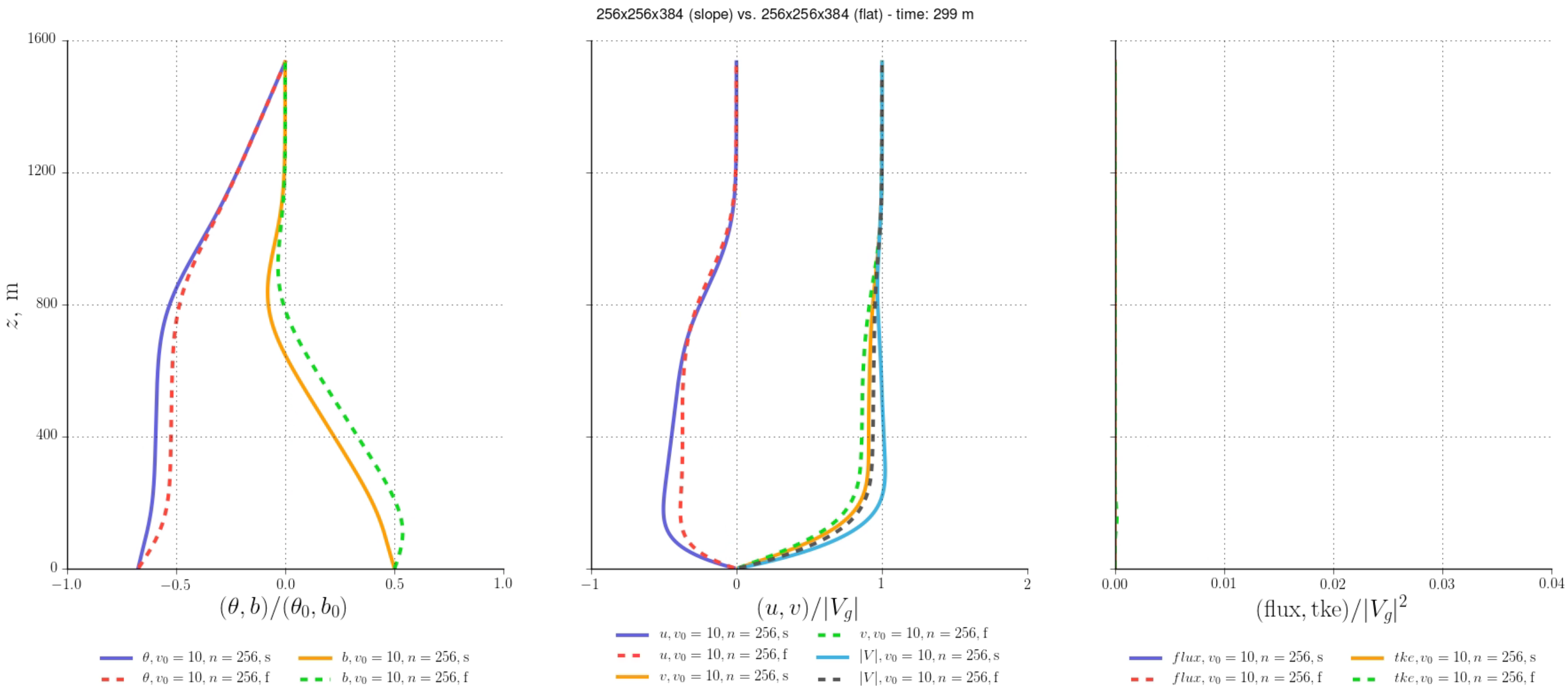

256x256x384 (slope) vs. 256x256x384 (flat) - time: 299 m
z, m
1600
1200
800
400
0
−1.0
−0.5
0.0
0.5
1.0
(θ, b)/(θ0, b0)
θ, v0 = 10, n = 256, s
θ, v0 = 10, n = 256, f
b, v0 = 10, n = 256, s
b, v0 = 10, n = 256, f
−1
0
1
2
(u, v)/|Vg|
u, v0 = 10, n = 256, s
u, v0 = 10, n = 256, f
v, v0 = 10, n = 256, s
v, v0 = 10, n = 256, f
|V|, v0 = 10, n = 256, s
|V|, v0 = 10, n = 256, f
0.00
0.01
0.02
0.03
0.04
(flux, tke)/|Vg|^2
flux, v0 = 10, n = 256, s
flux, v0 = 10, n = 256, f
tke, v0 = 10, n = 256, s
tke, v0 = 10, n = 256, f

256x256x384 (slope) vs. 256x256x384 (flat) - time: 360 m

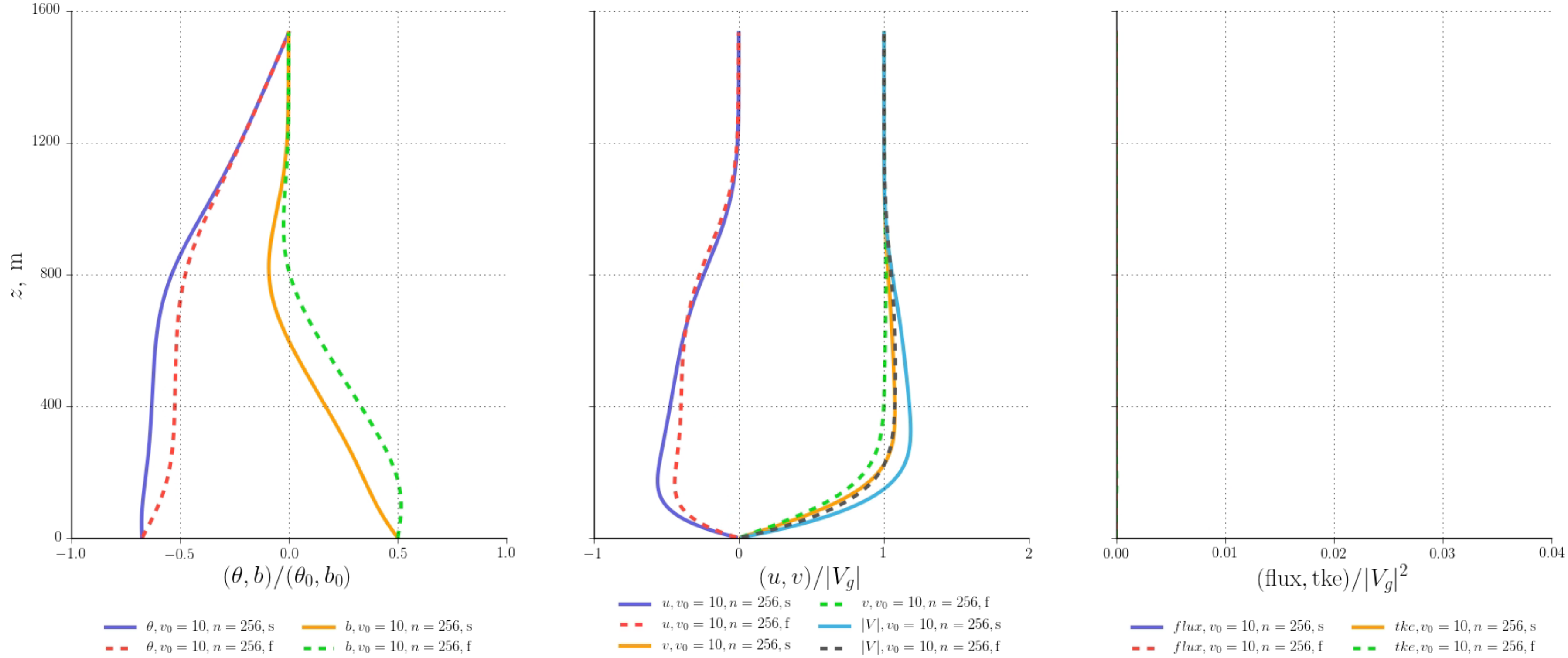

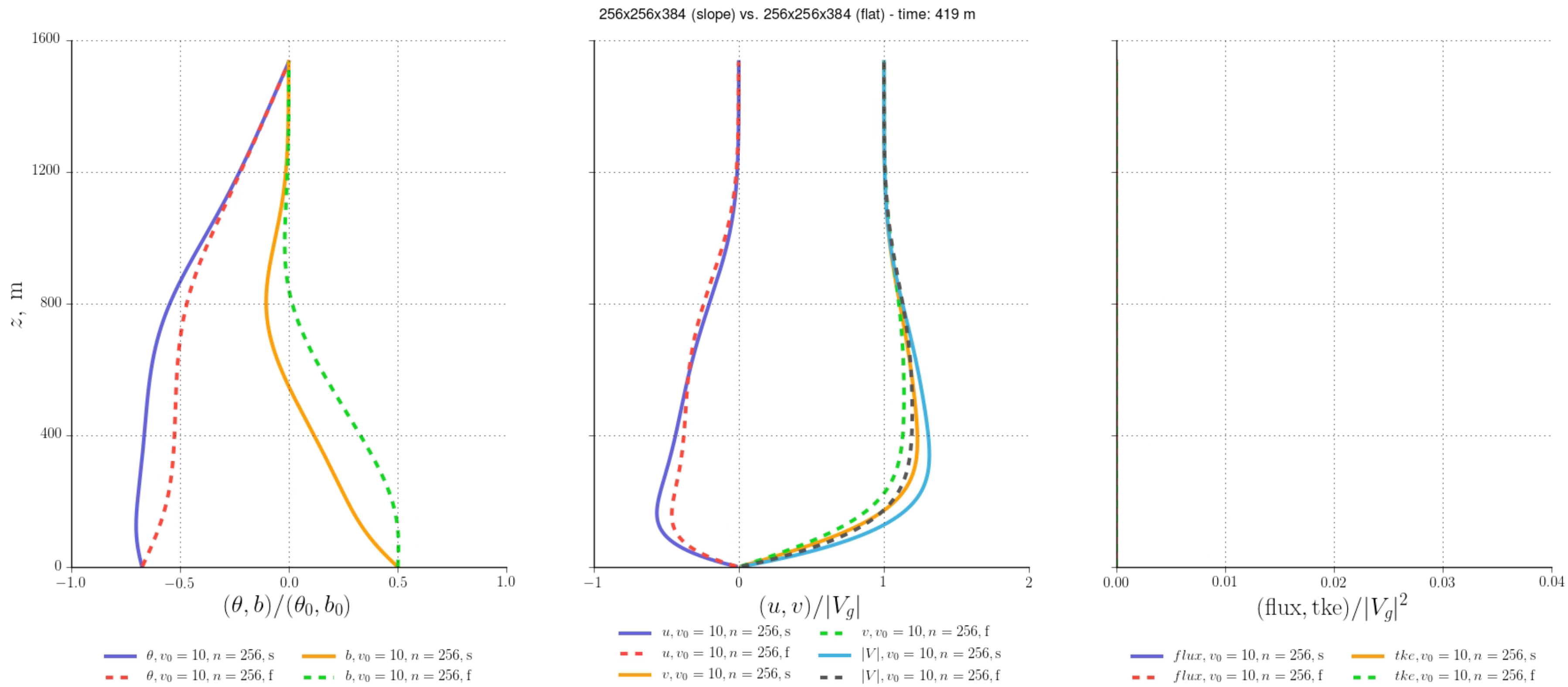
256x256x384 (slope) vs. 256x256x384 (flat) - time: 419 m
z, m
1600
1200
800
400
0
−1.0
−0.5
0.0
0.5
1.0
(θ, b)/(θ0, b0)
θ, v0 = 10, n = 256, s
θ, v0 = 10, n = 256, f
b, v0 = 10, n = 256, s
b, v0 = 10, n = 256, f
−1
0
1
2
(u, v)/|Vg|
u, v0 = 10, n = 256, s
u, v0 = 10, n = 256, f
v, v0 = 10, n = 256, s
v, v0 = 10, n = 256, f
|V|, v0 = 10, n = 256, s
|V|, v0 = 10, n = 256, f
0.00
0.01
0.02
0.03
0.04
(flux, tke)/|Vg|^2
flux, v0 = 10, n = 256, s
flux, v0 = 10, n = 256, f
tke, v0 = 10, n = 256, s
tke, v0 = 10, n = 256, f

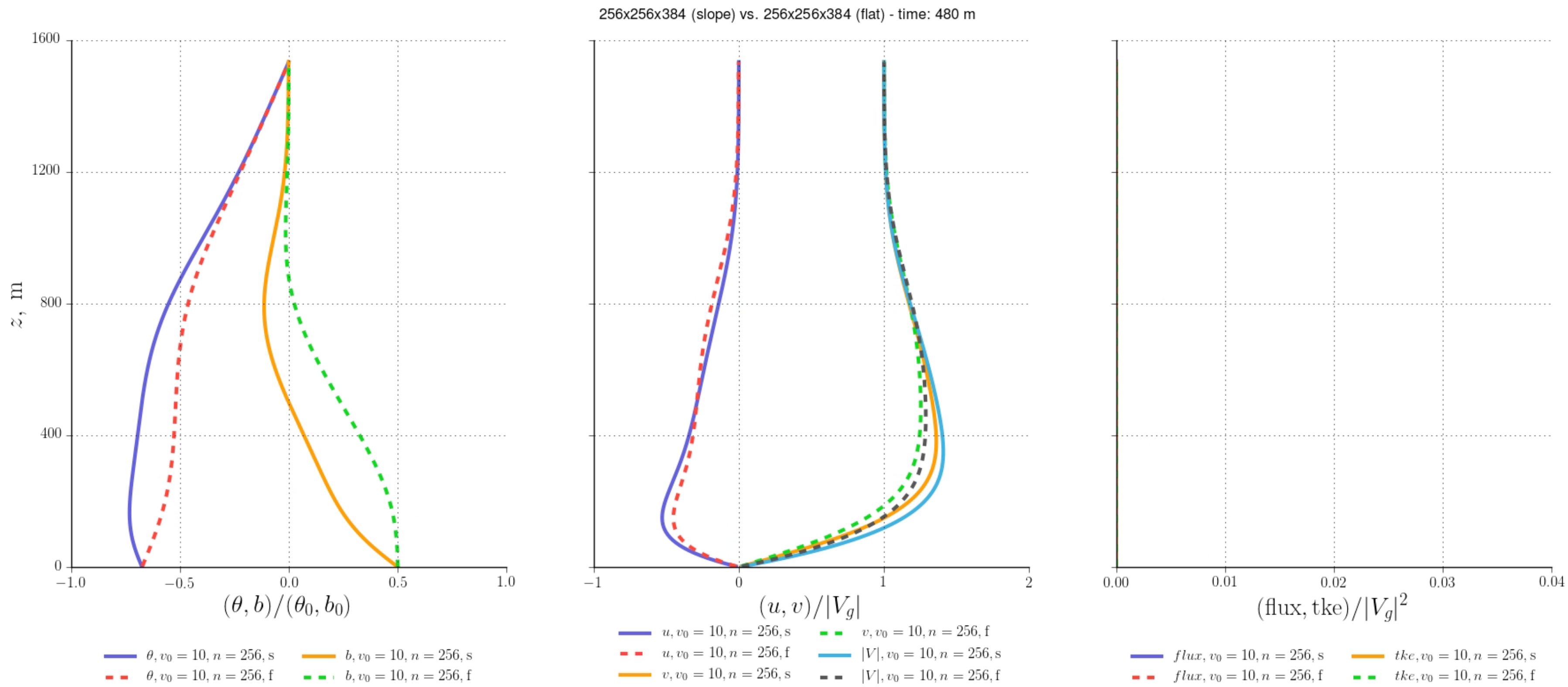

256x256x384 (slope) vs. 256x256x384 (flat) - time: 480 m
z, m
$(\theta, b)/(\theta_0, b_0)$
$\theta, v_0 = 10, n = 256$, s
$\theta, v_0 = 10, n = 256$, f
$b, v_0 = 10, n = 256$, s
$b, v_0 = 10, n = 256$, f
$(u, v)/|V_g|$
$u, v_0 = 10, n = 256$, s
$u, v_0 = 10, n = 256$, f
$v, v_0 = 10, n = 256$, s
$v, v_0 = 10, n = 256$, f
$|V|, v_0 = 10, n = 256$, s
$|V|, v_0 = 10, n = 256$, f
$(\mathrm{flux}, \mathrm{tke})/|V_g|^2$
$flux, v_0 = 10, n = 256$, s
$flux, v_0 = 10, n = 256$, f
$tke, v_0 = 10, n = 256$, s
$tke, v_0 = 10, n = 256$, f

256x256x384 (slope) vs. 256x256x384 (flat) - time: 541 m

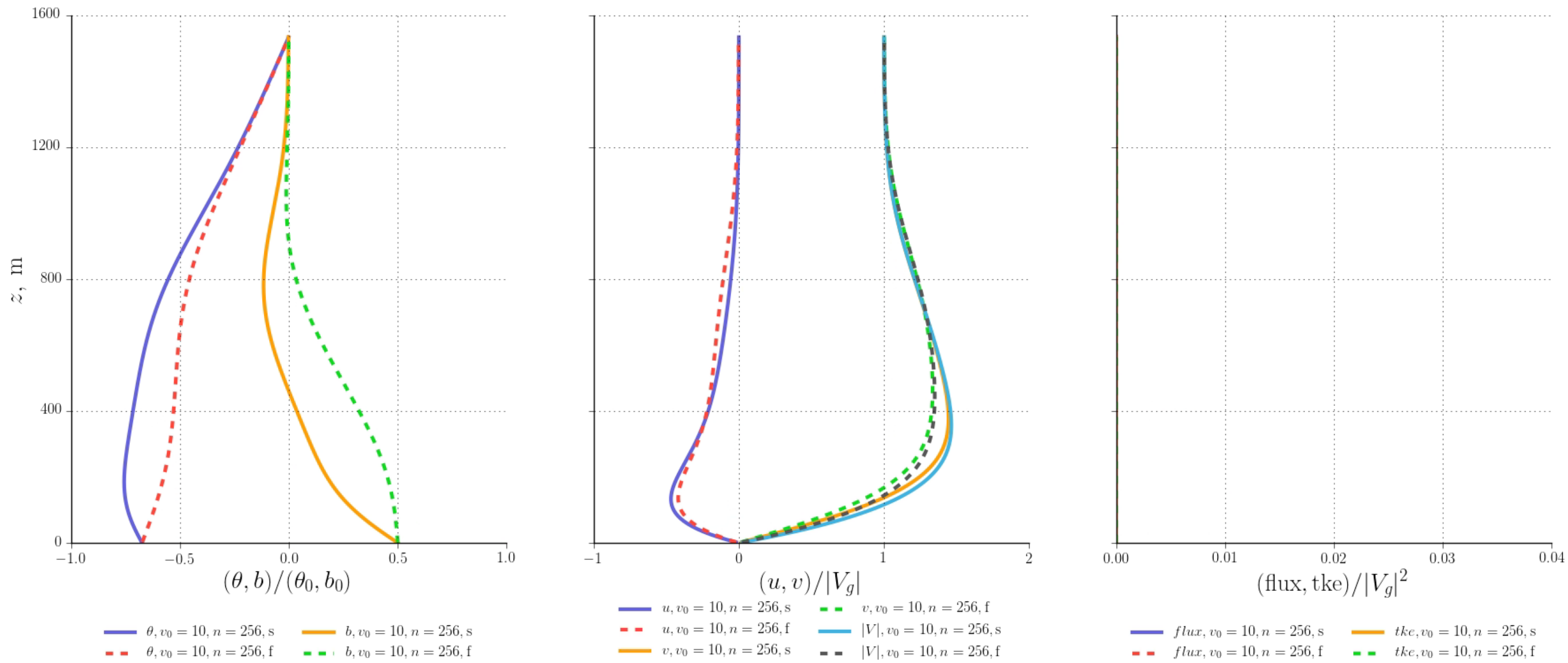

256x256x384 (slope) vs. 256x256x384 (flat) - time: 599 m

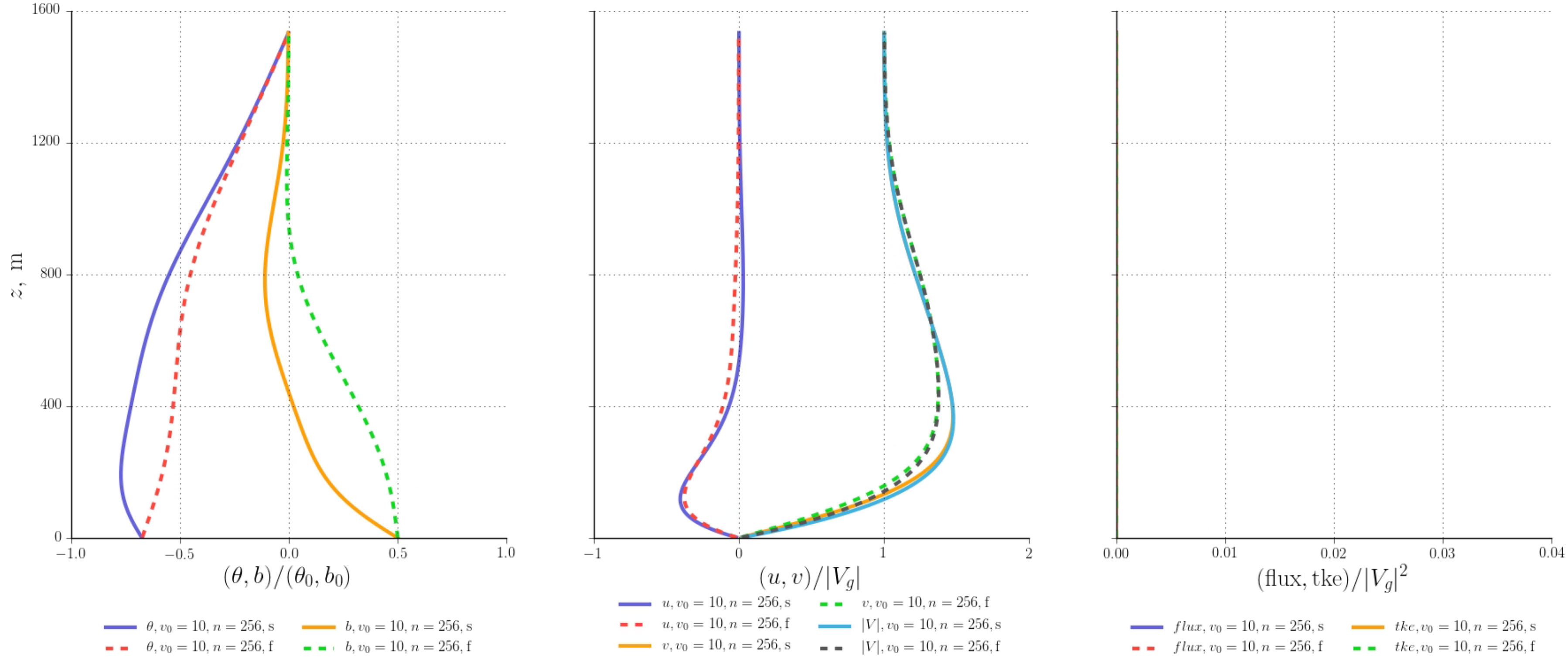

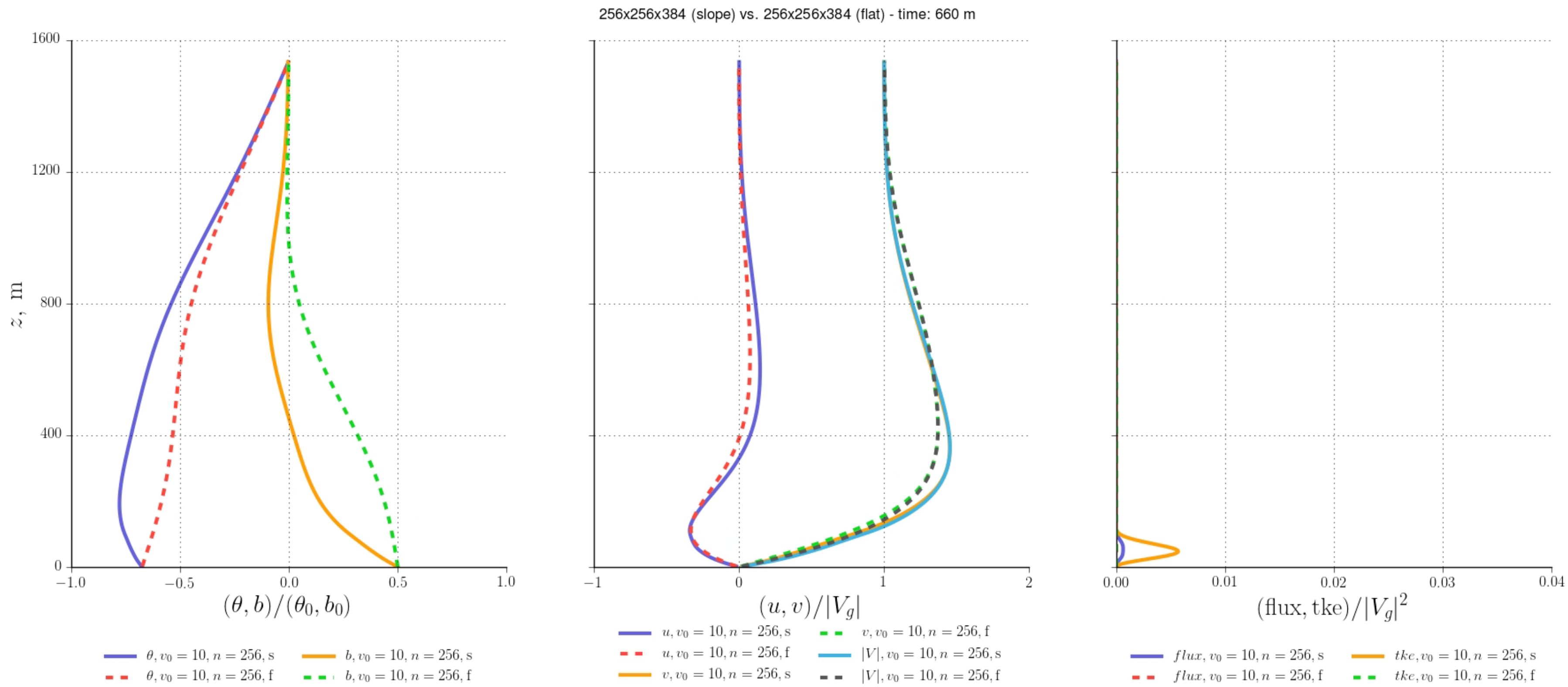
256x256x384 (slope) vs. 256x256x384 (flat) - time: 660 m
z, m
1600
1200
800
400
0
−1.0
−0.5
0.0
0.5
1.0
$(\theta, b)/(\theta_0, b_0)$
$\theta, v_0 = 10, n = 256$, s
$\theta, v_0 = 10, n = 256$, f
$b, v_0 = 10, n = 256$, s
$b, v_0 = 10, n = 256$, f
−1
0
1
2
$(u, v)/|V_g|$
$u, v_0 = 10, n = 256$, s
$u, v_0 = 10, n = 256$, f
$v, v_0 = 10, n = 256$, s
$v, v_0 = 10, n = 256$, f
$|V|, v_0 = 10, n = 256$, s
$|V|, v_0 = 10, n = 256$, f
0.00
0.01
0.02
0.03
0.04
$(\text{flux}, \text{tke})/|V_g|^2$
$flux, v_0 = 10, n = 256$, s
$flux, v_0 = 10, n = 256$, f
$tke, v_0 = 10, n = 256$, s
$tke, v_0 = 10, n = 256$, f

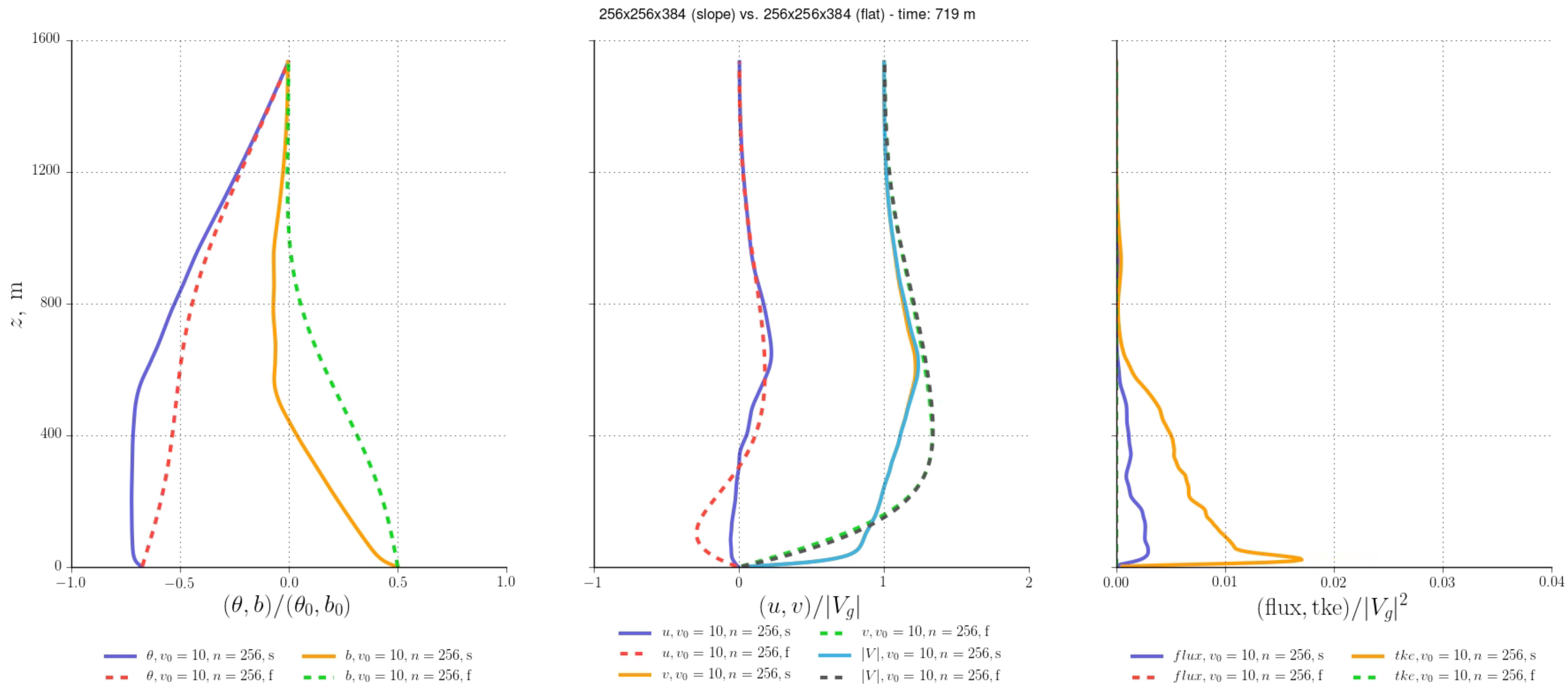
256x256x384 (slope) vs. 256x256x384 (flat) - time: 719 m
z, m
$(\theta, b)/(\theta_0, b_0)$
$(u, v)/|V_g|$
$(\mathrm{flux}, \mathrm{tke})/|V_g|^2$
$\theta, v_0 = 10, n = 256$, s
$\theta, v_0 = 10, n = 256$, f
$b, v_0 = 10, n = 256$, s
$b, v_0 = 10, n = 256$, f
$u, v_0 = 10, n = 256$, s
$u, v_0 = 10, n = 256$, f
$v, v_0 = 10, n = 256$, s
$v, v_0 = 10, n = 256$, f
$|V|, v_0 = 10, n = 256$, s
$|V|, v_0 = 10, n = 256$, f
$flux, v_0 = 10, n = 256$, s
$flux, v_0 = 10, n = 256$, f
$tke, v_0 = 10, n = 256$, s
$tke, v_0 = 10, n = 256$, f

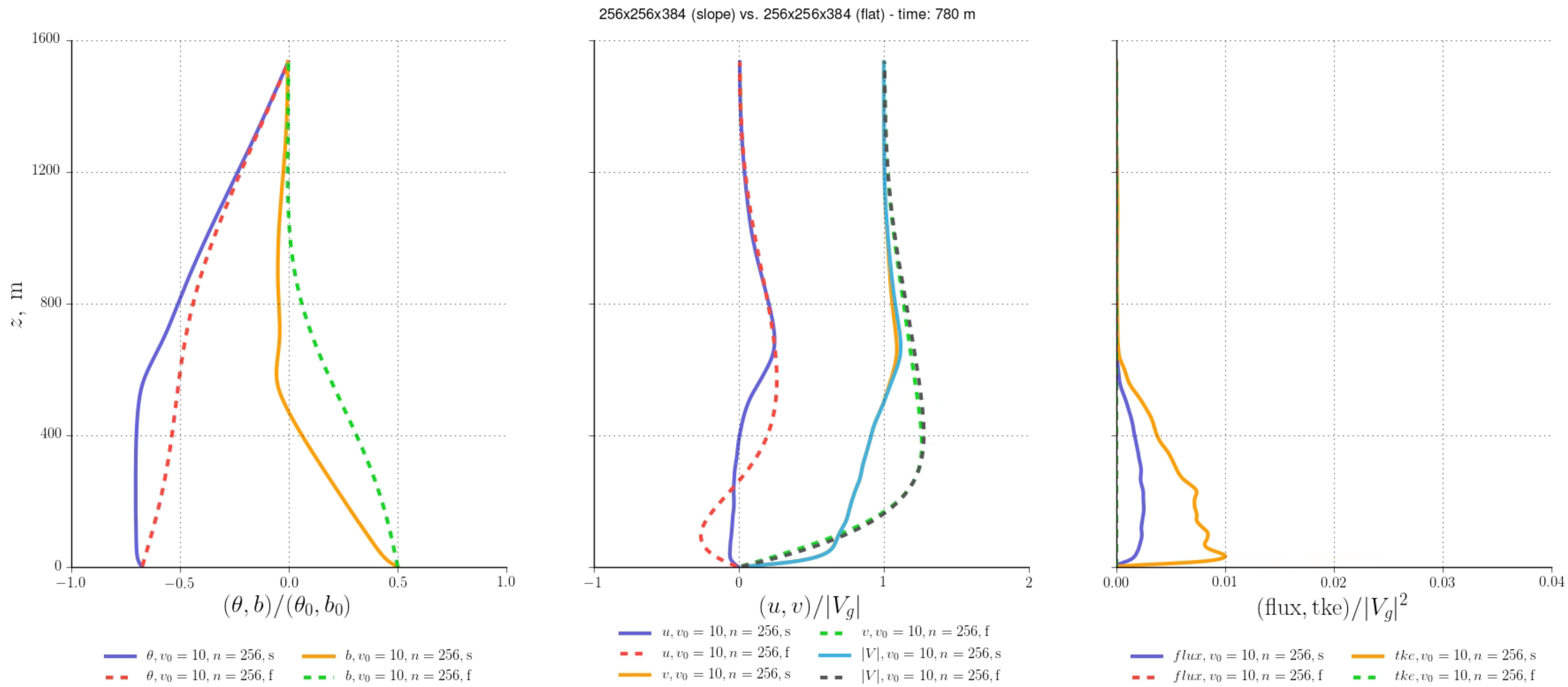
256x256x384 (slope) vs. 256x256x384 (flat) - time: 780 m
1600
1200
800
400
0
z, m
−1.0
−0.5
0.0
0.5
1.0
$(\theta, b)/(\theta_0, b_0)$
$\theta, v_0 = 10, n = 256$, s
$\theta, v_0 = 10, n = 256$, f
$b, v_0 = 10, n = 256$, s
$b, v_0 = 10, n = 256$, f
−1
0
1
2
$(u, v)/|V_g|$
$u, v_0 = 10, n = 256$, s
$u, v_0 = 10, n = 256$, f
$v, v_0 = 10, n = 256$, s
$v, v_0 = 10, n = 256$, f
$|V|, v_0 = 10, n = 256$, s
$|V|, v_0 = 10, n = 256$, f
0.00
0.01
0.02
0.03
0.04
$(\text{flux}, \text{tke})/|V_g|^2$
$flux, v_0 = 10, n = 256$, s
$flux, v_0 = 10, n = 256$, f
$tke, v_0 = 10, n = 256$, s
$tke, v_0 = 10, n = 256$, f

256x256x384 (slope) vs. 256x256x384 (flat) - time: 841 m

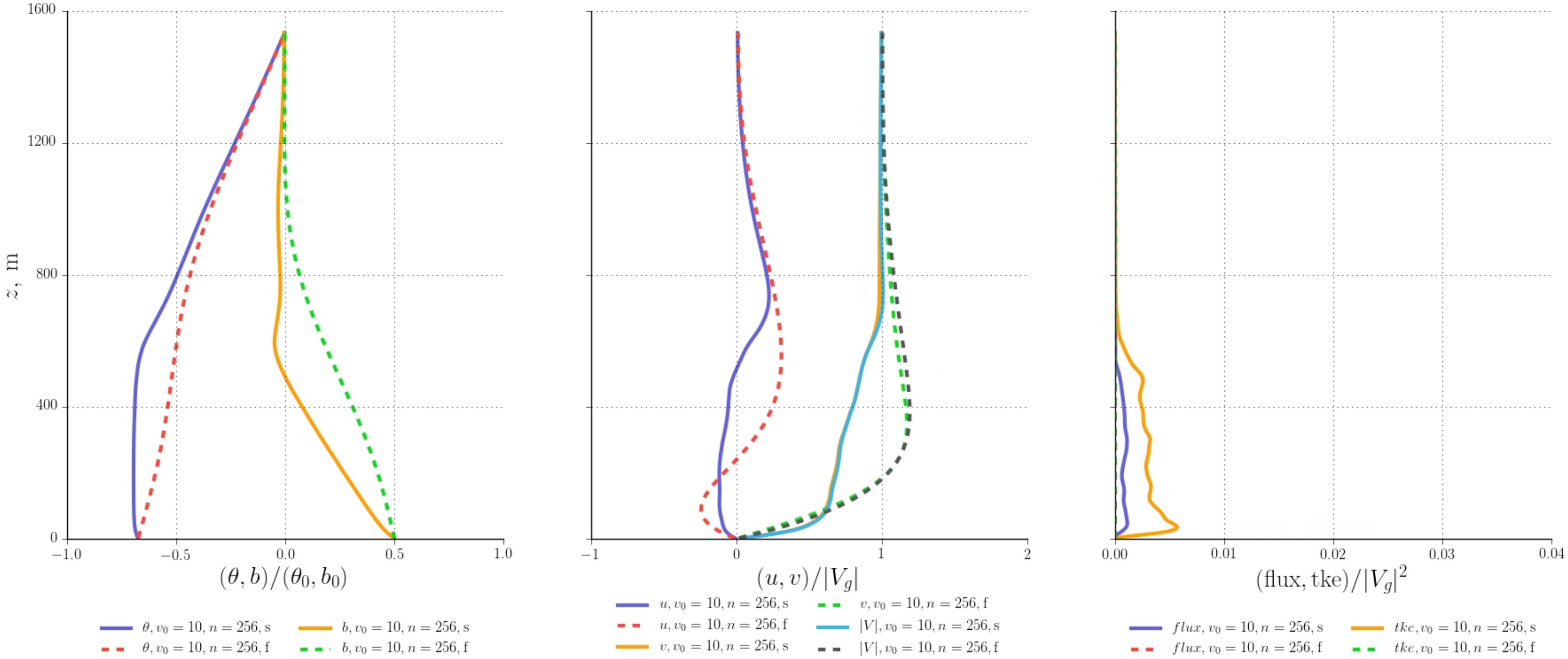

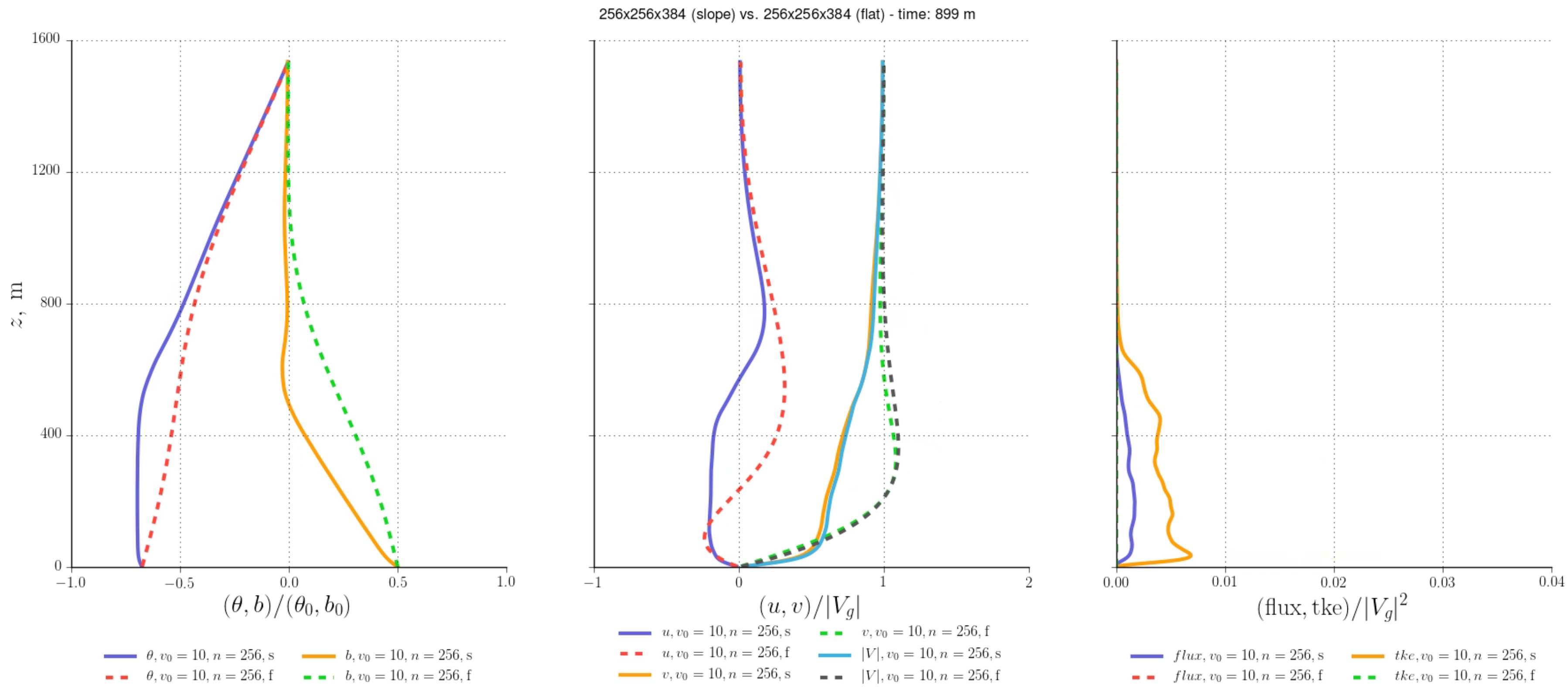
256x256x384 (slope) vs. 256x256x384 (flat) - time: 899 m
z, m
$(\theta, b)/(\theta_0, b_0)$
$\theta, v_0 = 10, n = 256$, s
$\theta, v_0 = 10, n = 256$, f
$b, v_0 = 10, n = 256$, s
$b, v_0 = 10, n = 256$, f
$(u, v)/|V_g|$
$u, v_0 = 10, n = 256$, s
$u, v_0 = 10, n = 256$, f
$v, v_0 = 10, n = 256$, s
$v, v_0 = 10, n = 256$, f
$|V|, v_0 = 10, n = 256$, s
$|V|, v_0 = 10, n = 256$, f
$(\text{flux}, \text{tke})/|V_g|^2$
$flux, v_0 = 10, n = 256$, s
$flux, v_0 = 10, n = 256$, f
$tke, v_0 = 10, n = 256$, s
$tke, v_0 = 10, n = 256$, f

Slope-angle sensitivity of TKE and V: α = 0º, 0.09º, 0.18º, 0.27º

Surface buoyancy flux forcing case

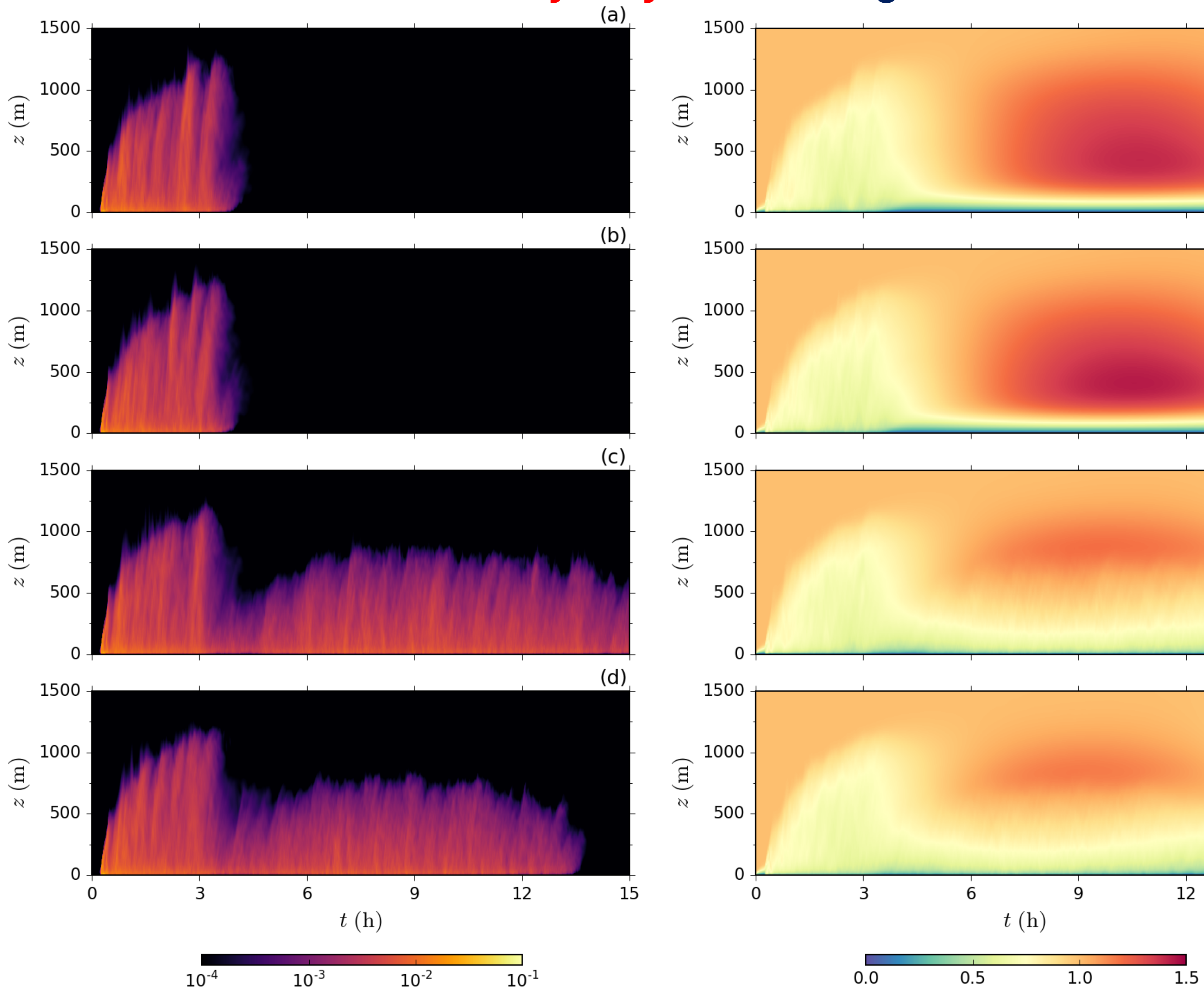

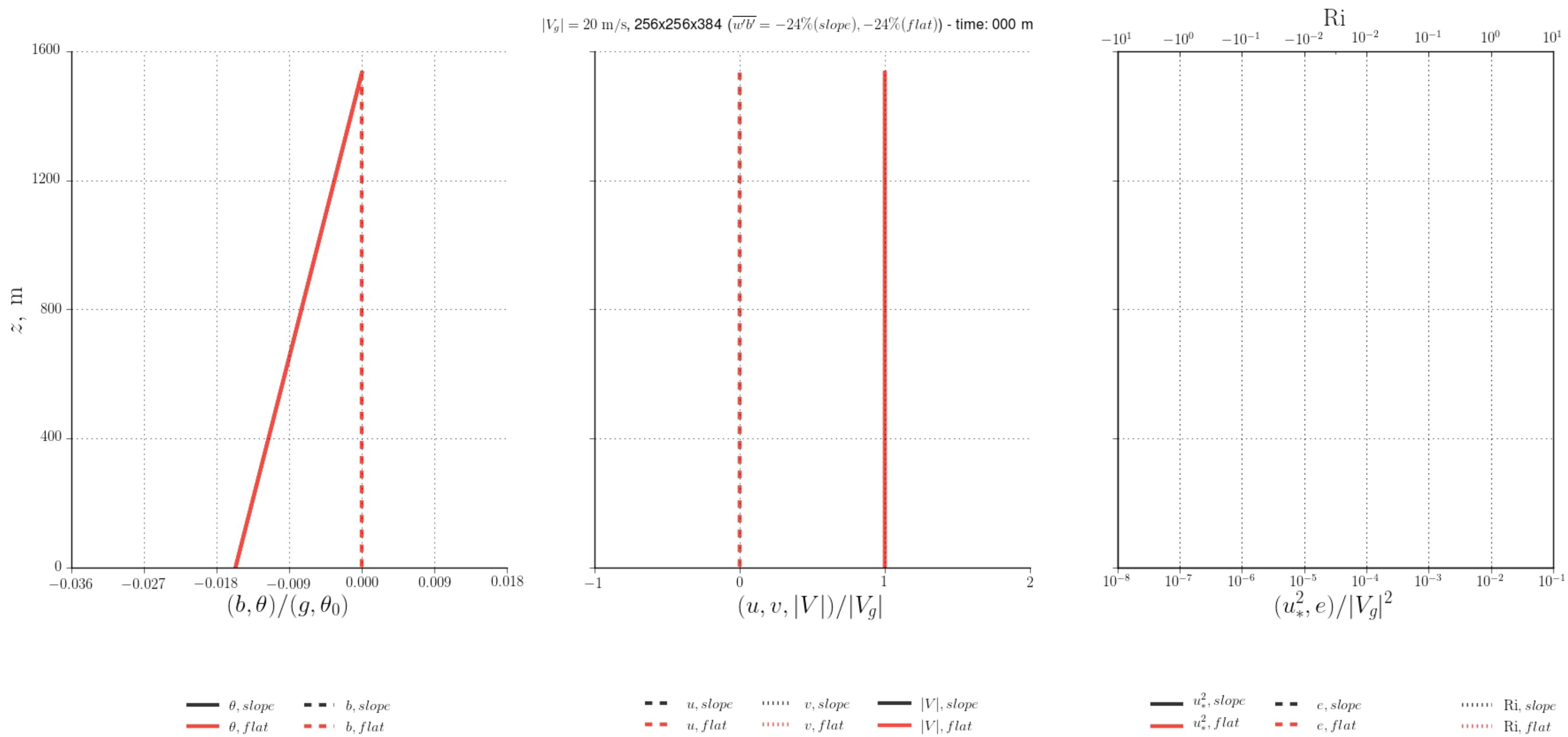

$|V_g| = 20$ m/s, 256x256x384 ($\overline{w'b'} = -24\%(slope), -24\%(flat)$) - time: 000 m
z, m
$(b, \theta)/(g, \theta_0)$
$(u, v, |V|)/|V_g|$
Ri
$(u_*^2, e)/|V_g|^2$
θ, slope
θ, flat
b, slope
b, flat
u, slope
u, flat
v, slope
v, flat
$|V|$, slope
$|V|$, flat
u_*^2, slope
u_*^2, flat
e, slope
e, flat
Ri, slope
Ri, flat

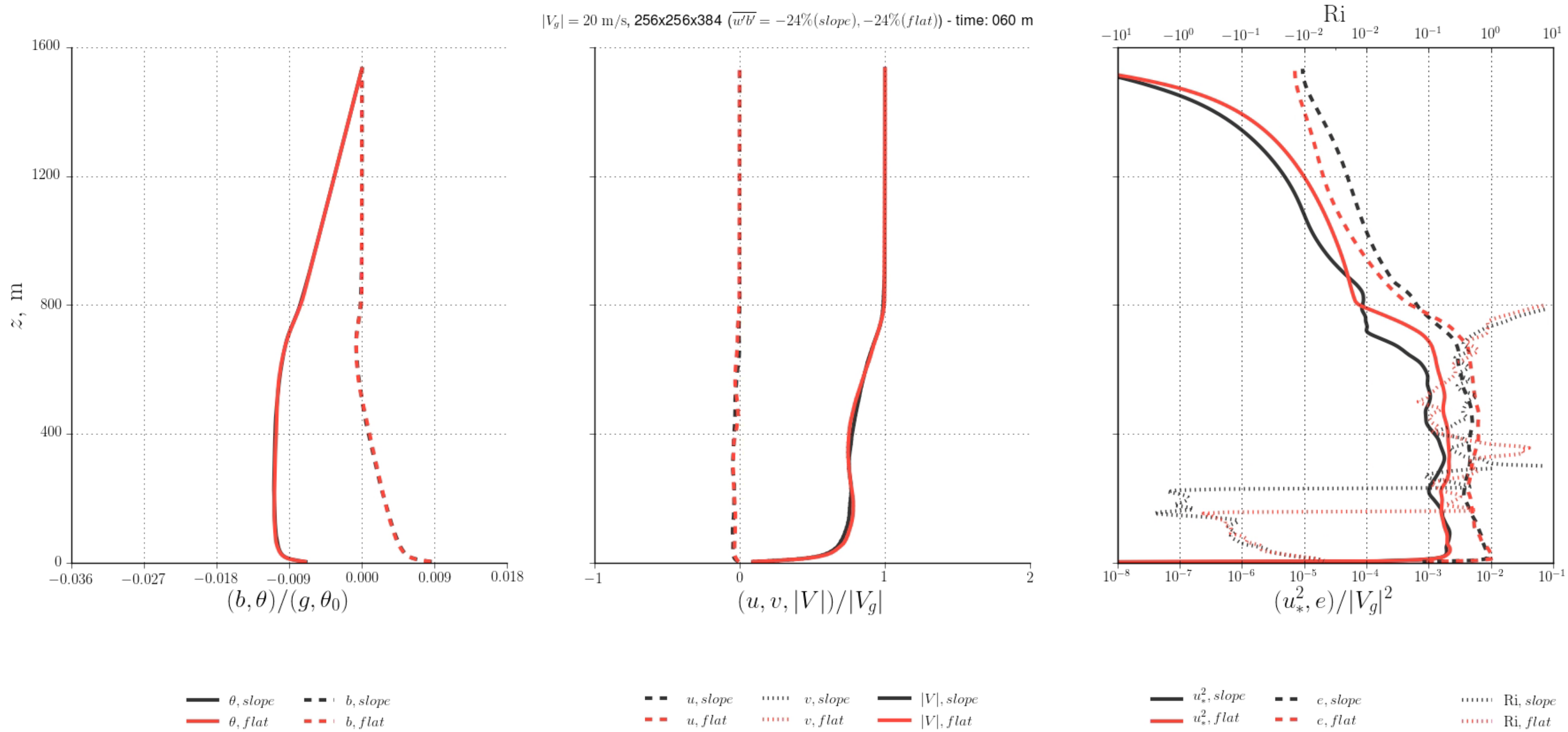

$|V_g| = 20$ m/s, 256x256x384 ($\overline{w'b'} = -24\%(slope), -24\%(flat)$) - time: 060 m
z, m
$(b,\theta)/(g,\theta_0)$
$(u, v, |V|)/|V_g|$
Ri
$(u_*^2, e)/|V_g|^2$
θ, slope
θ, flat
b, slope
b, flat
u, slope
u, flat
v, slope
v, flat
$|V|$, slope
$|V|$, flat
u_*^2, slope
u_*^2, flat
e, slope
e, flat
Ri, slope
Ri, flat

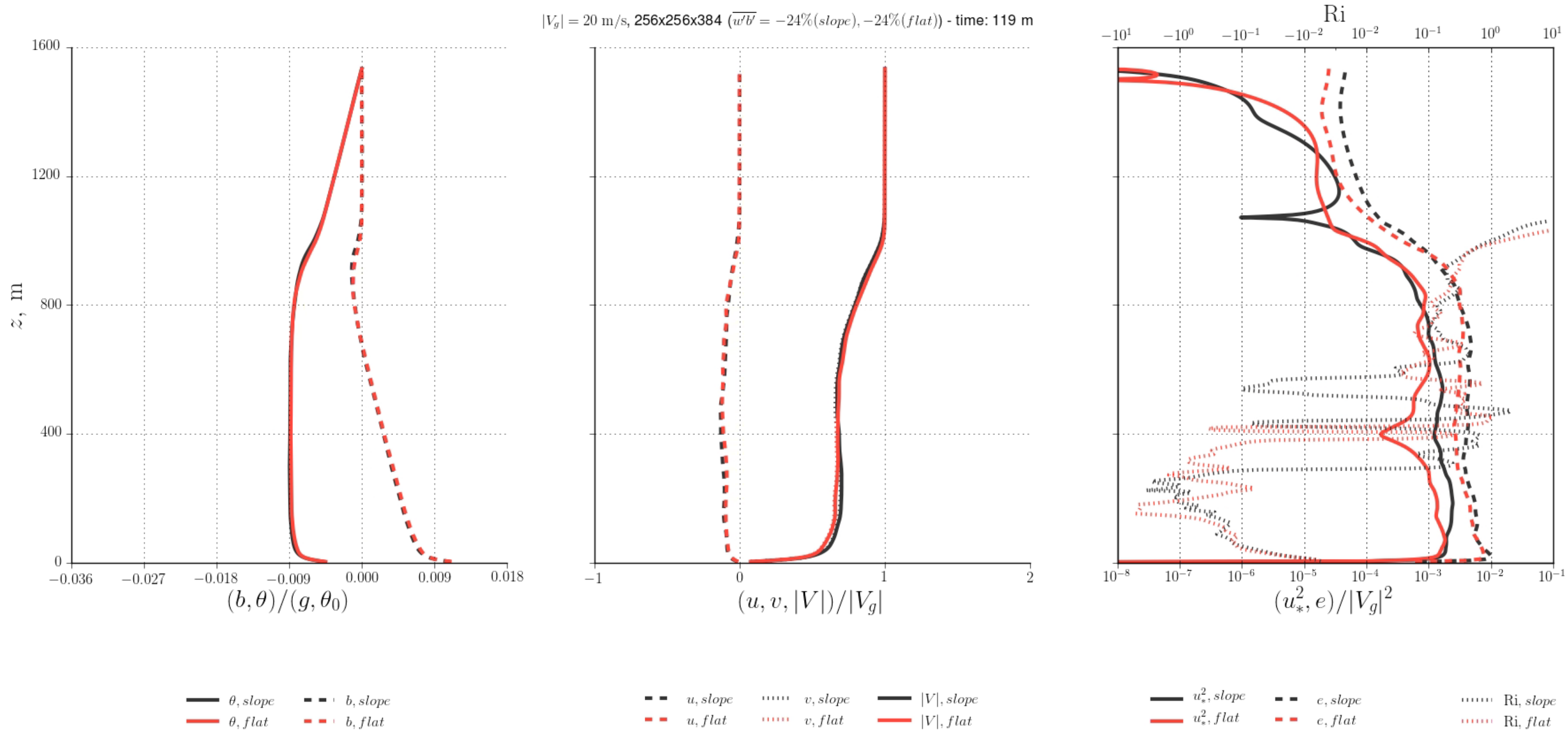

$|V_g| = 20$ m/s, 256x256x384 ($\overline{w'b'} = -24\%(slope), -24\%(flat)$) - time: 119 m
z, m
$(b, \theta)/(g, \theta_0)$
$(u, v, |V|)/|V_g|$
$(u_*^2, e)/|V_g|^2$
Ri
$\theta, slope$
$\theta, flat$
$b, slope$
$b, flat$
$u, slope$
$u, flat$
$v, slope$
$v, flat$
$|V|, slope$
$|V|, flat$
$u_*^2, slope$
$u_*^2, flat$
$e, slope$
$e, flat$
Ri, $slope$
Ri, $flat$

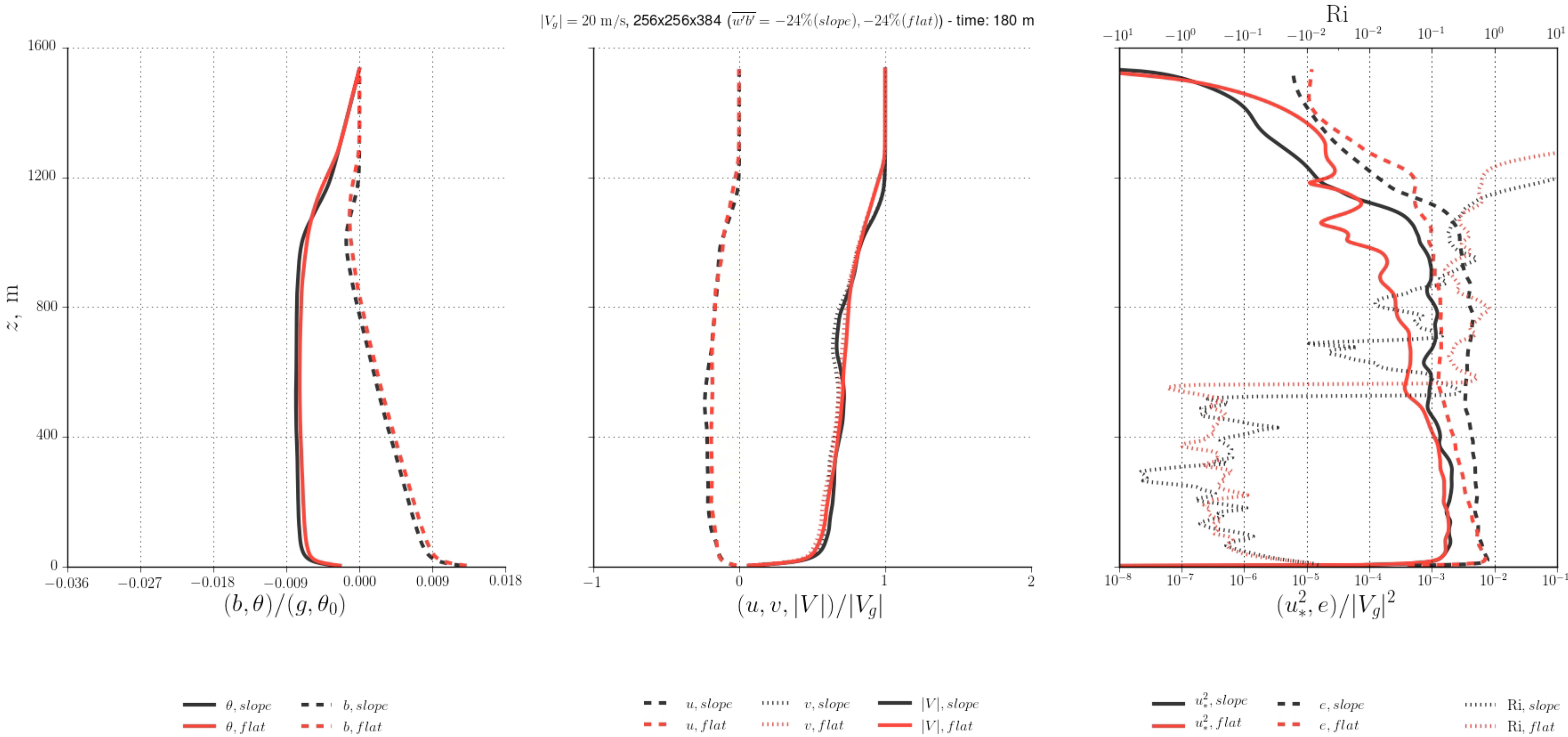

$|V_g| = 20$ m/s, 256x256x384 ($\overline{w'b'} = -24\%(slope), -24\%(flat)$) - time: 180 m
1600
1200
800
400
0
z, m
−0.036
−0.027
−0.018
−0.009
0.000
0.009
0.018
$(b, \theta)/(g, \theta_0)$
−1
0
1
2
$(u, v, |V|)/|V_g|$
Ri
-10^1
-10^0
-10^{-1}
-10^{-2}
10^{-2}
10^{-1}
10^0
10^1
10^{-8}
10^{-7}
10^{-6}
10^{-5}
10^{-4}
10^{-3}
10^{-2}
10^{-1}
$(u_*^2, e)/|V_g|^2$
θ, $slope$
θ, $flat$
b, $slope$
b, $flat$
u, $slope$
u, $flat$
v, $slope$
v, $flat$
$|V|$, $slope$
$|V|$, $flat$
u_*^2, $slope$
u_*^2, $flat$
e, $slope$
e, $flat$
Ri, $slope$
Ri, $flat$

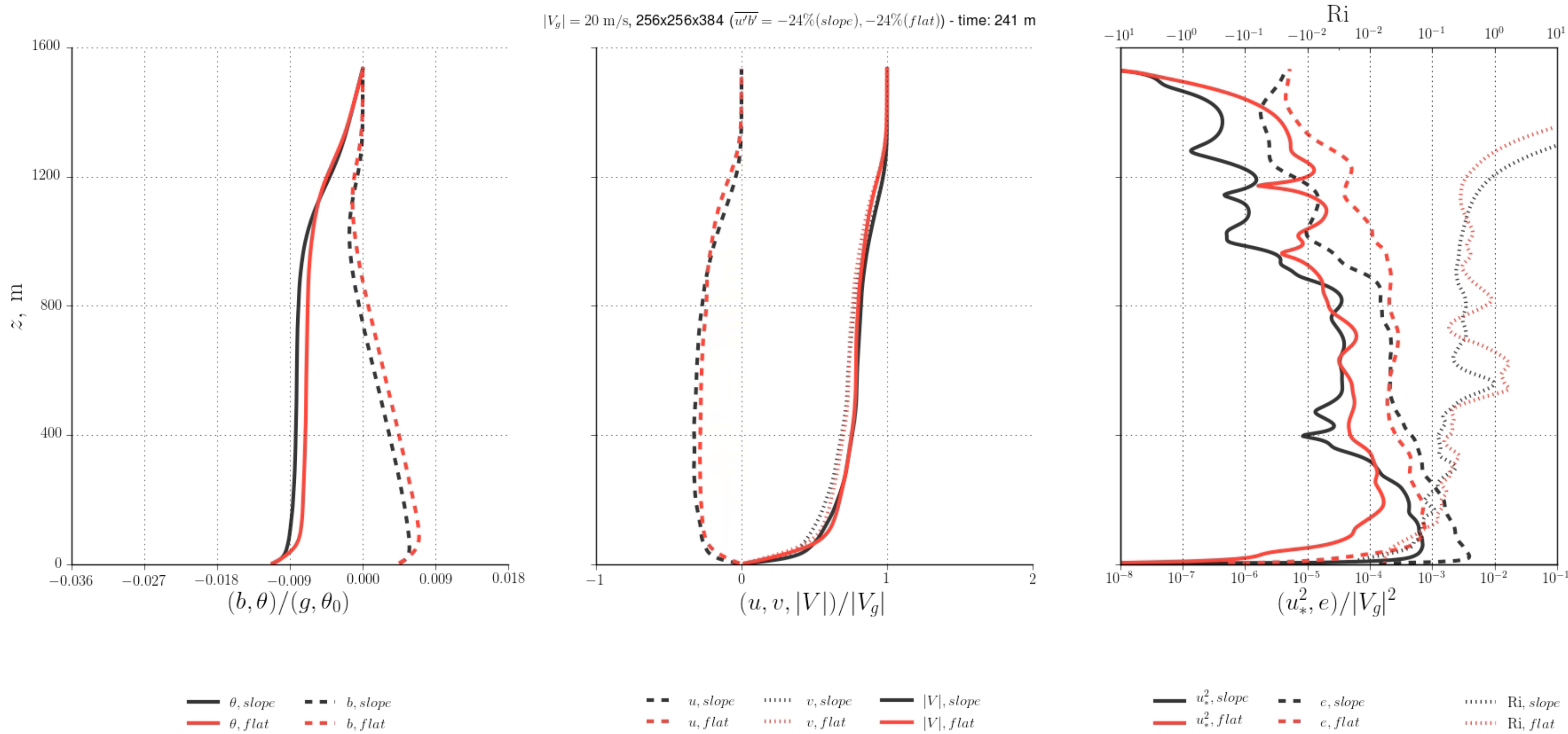

$|V_g| = 20$ m/s, 256x256x384 ($\overline{w'b'} = -24\%(slope), -24\%(flat)$) - time: 241 m
z, m
$(b, \theta)/(g, \theta_0)$
$(u, v, |V|)/|V_g|$
Ri
$(u_*^2, e)/|V_g|^2$
θ, *slope*
θ, *flat*
b, *slope*
b, *flat*
u, *slope*
u, *flat*
v, *slope*
v, *flat*
$|V|$, *slope*
$|V|$, *flat*
u_*^2, *slope*
u_*^2, *flat*
e, *slope*
e, *flat*
Ri, *slope*
Ri, *flat*

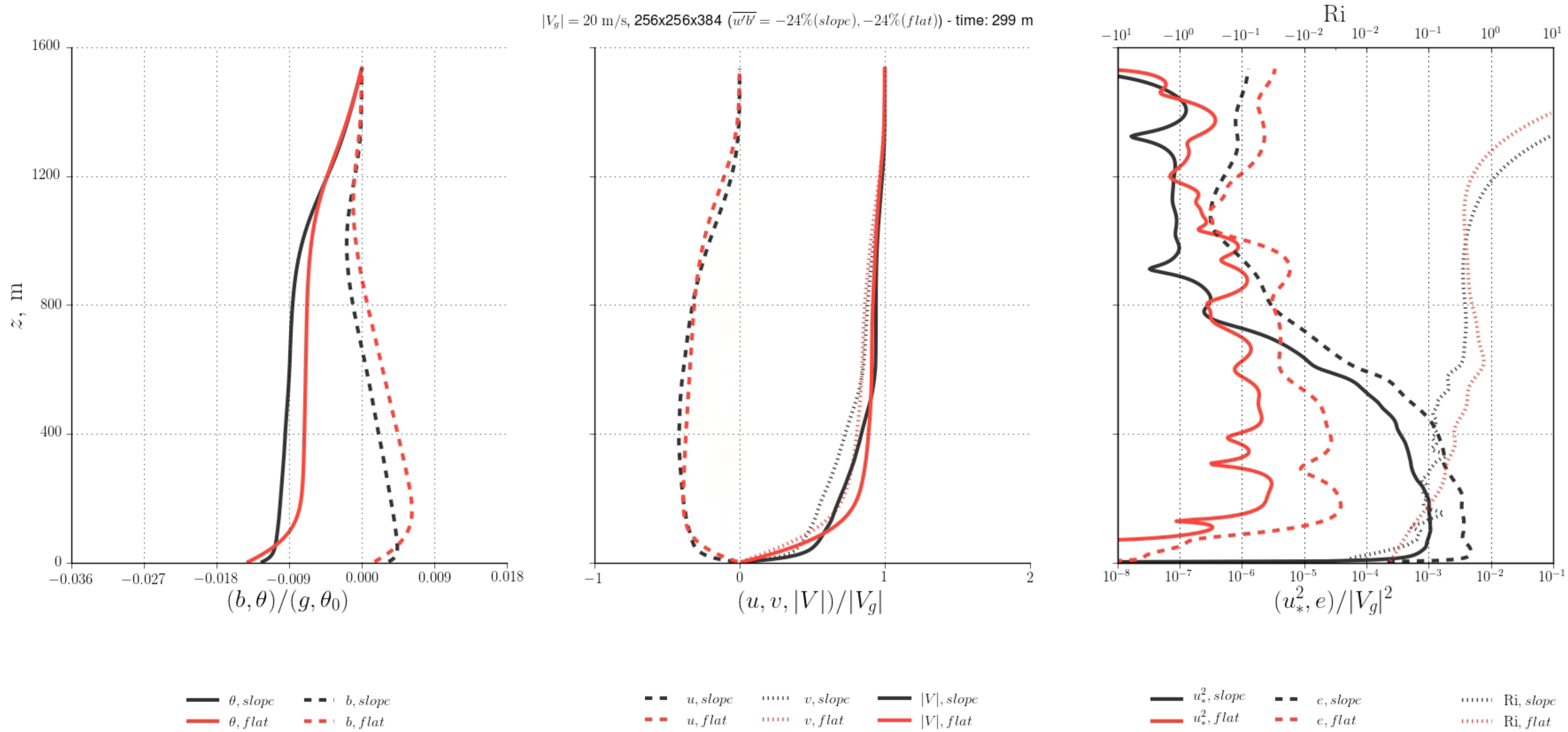
$|V_g| = 20$ m/s, 256x256x384 ($\overline{w'b'} = -24\%(slope), -24\%(flat)$) - time: 299 m
z, m
1600
1200
800
400
0
−0.036
−0.027
−0.018
−0.009
0.000
0.009
0.018
$(b,\theta)/(g,\theta_0)$
−1
0
1
2
$(u, v, |V|)/|V_g|$
Ri
-10^1
-10^0
-10^{-1}
-10^{-2}
10^{-2}
10^{-1}
10^0
10^1
10^{-8}
10^{-7}
10^{-6}
10^{-5}
10^{-4}
10^{-3}
10^{-2}
10^{-1}
$(u_*^2, e)/|V_g|^2$
θ, slope
θ, flat
b, slope
b, flat
u, slope
u, flat
v, slope
v, flat
$|V|$, slope
$|V|$, flat
u_*^2, slope
u_*^2, flat
e, slope
e, flat
Ri, slope
Ri, flat

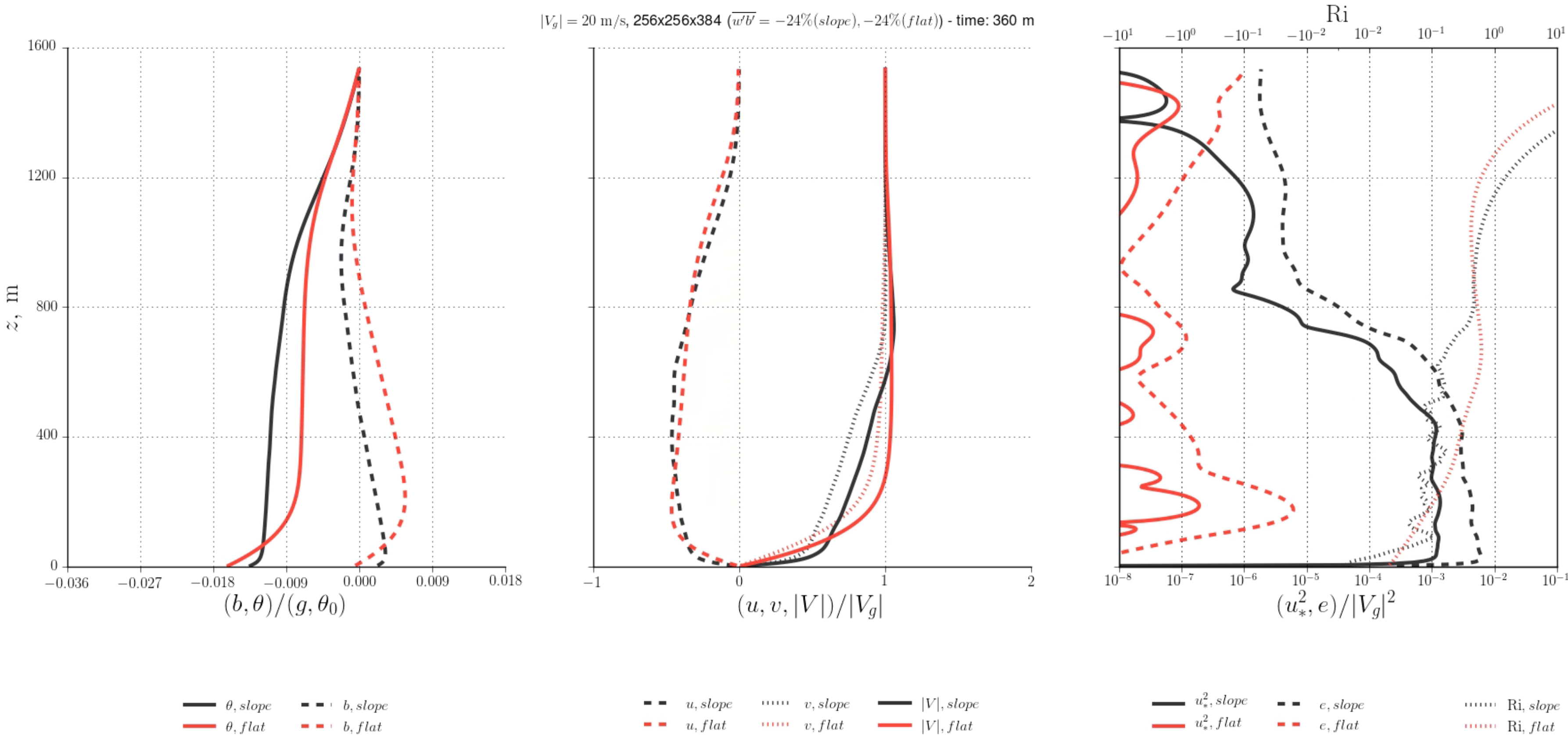

|Vg| = 20 m/s, 256x256x384 (w'b' = −24%(slope), −24%(flat)) - time: 360 m
z, m
(b, θ)/(g, θ0)
(u, v, |V|)/|Vg|
(u*², e)/|Vg|²
Ri
θ, slope
θ, flat
b, slope
b, flat
u, slope
u, flat
v, slope
v, flat
|V|, slope
|V|, flat
u*², slope
u*², flat
e, slope
e, flat
Ri, slope
Ri, flat

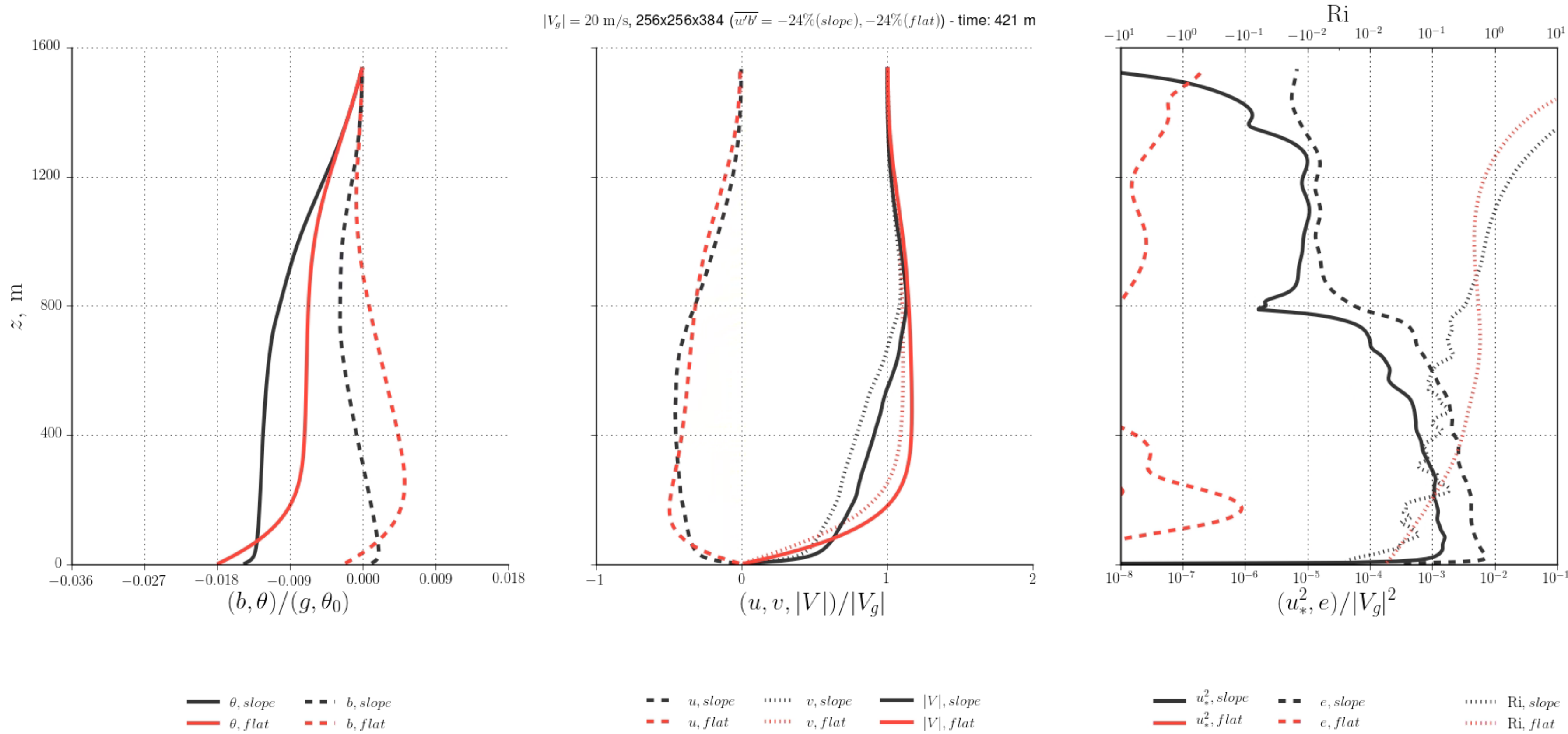
$|V_g| = 20$ m/s, 256x256x384 ($\overline{w'b'} = -24\%(slope), -24\%(flat)$) - time: 421 m
z, m
$(b, \theta)/(g, \theta_0)$
$(u, v, |V|)/|V_g|$
Ri
$(u_*^2, e)/|V_g|^2$
θ, slope
θ, flat
b, slope
b, flat
u, slope
u, flat
v, slope
v, flat
$|V|$, slope
$|V|$, flat
u_*^2, slope
u_*^2, flat
e, slope
e, flat
Ri, slope
Ri, flat

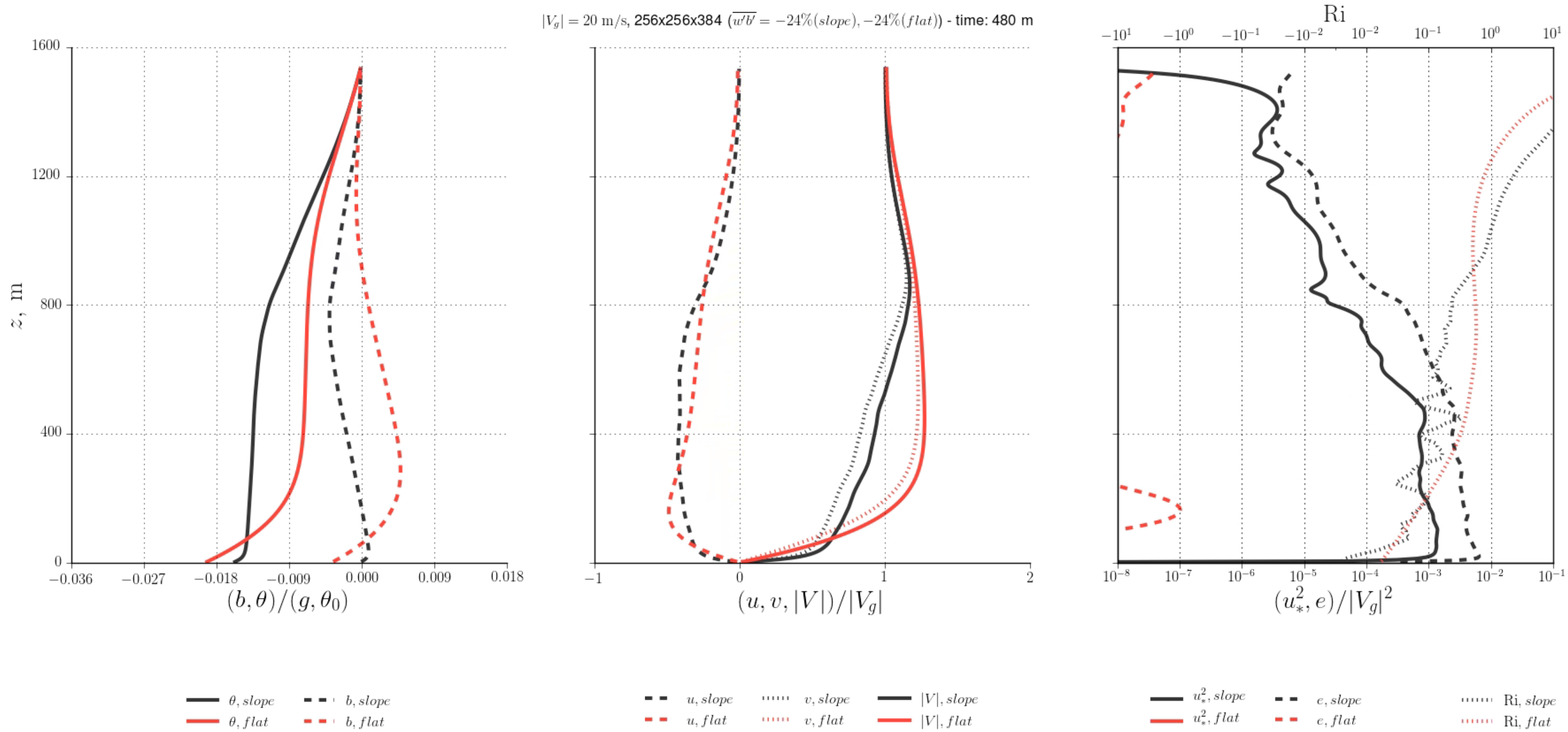

$|V_g| = 20$ m/s, 256x256x384 ($\overline{w'b'} = -24\%(slope), -24\%(flat)$) - time: 480 m
z, m
1600
1200
800
400
0
−0.036
−0.027
−0.018
−0.009
0.000
0.009
0.018
$(b, \theta)/(g, \theta_0)$
−1
0
1
2
$(u, v, |V|)/|V_g|$
Ri
-10^1
-10^0
-10^{-1}
-10^{-2}
10^{-2}
10^{-1}
10^0
10^1
10^{-8}
10^{-7}
10^{-6}
10^{-5}
10^{-4}
10^{-3}
10^{-2}
10^{-1}
$(u_*^2, e)/|V_g|^2$
θ, slope
θ, flat
b, slope
b, flat
u, slope
u, flat
v, slope
v, flat
|V|, slope
|V|, flat
u_*^2, slope
u_*^2, flat
e, slope
e, flat
Ri, slope
Ri, flat

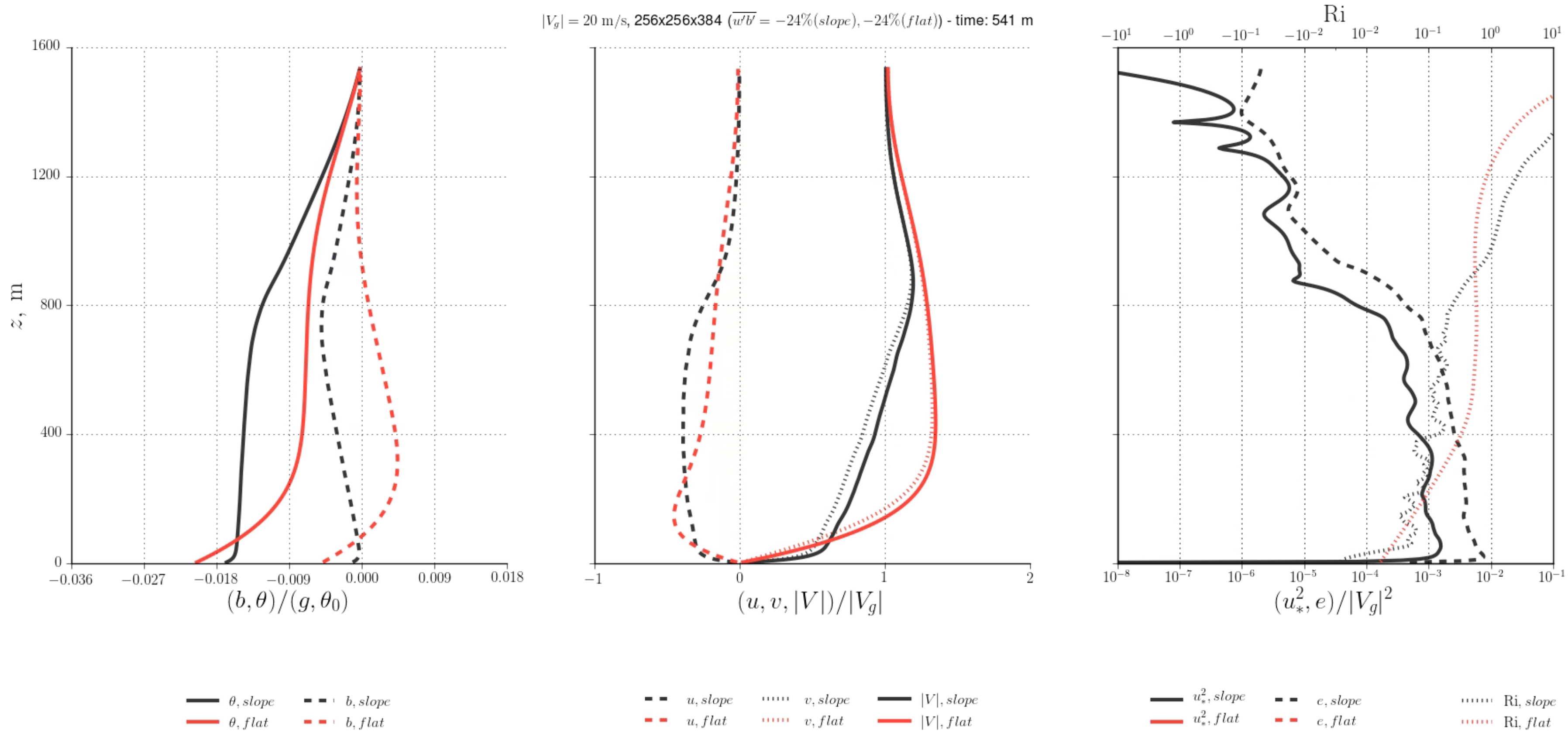

$|V_g| = 20$ m/s, 256x256x384 ($\overline{w'b'} = -24\%(slope), -24\%(flat)$) - time: 541 m
z, m
$(b, \theta)/(g, \theta_0)$
$(u, v, |V|)/|V_g|$
$(u_*^2, e)/|V_g|^2$
Ri
θ, $slope$
θ, $flat$
b, $slope$
b, $flat$
u, $slope$
u, $flat$
v, $slope$
v, $flat$
$|V|$, $slope$
$|V|$, $flat$
u_*^2, $slope$
u_*^2, $flat$
e, $slope$
e, $flat$
Ri, $slope$
Ri, $flat$

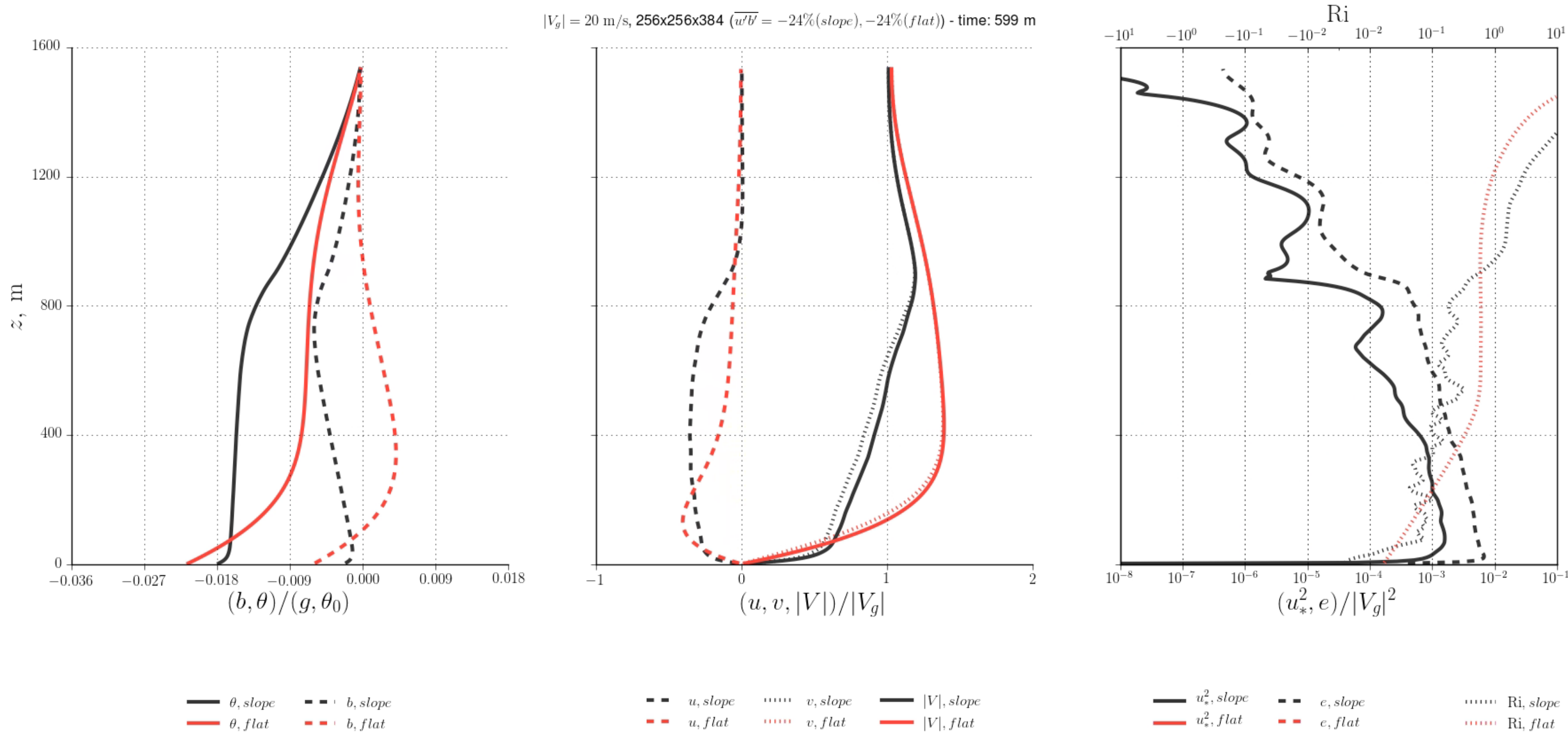

$|V_g| = 20$ m/s, 256x256x384 ($\overline{w'b'} = -24\%(slope), -24\%(flat)$) - time: 599 m
z, m
$(b, \theta)/(g, \theta_0)$
$(u, v, |V|)/|V_g|$
Ri
$(u_*^2, e)/|V_g|^2$
θ, slope
θ, flat
b, slope
b, flat
u, slope
u, flat
v, slope
v, flat
$|V|$, slope
$|V|$, flat
u_*^2, slope
u_*^2, flat
e, slope
e, flat
Ri, slope
Ri, flat

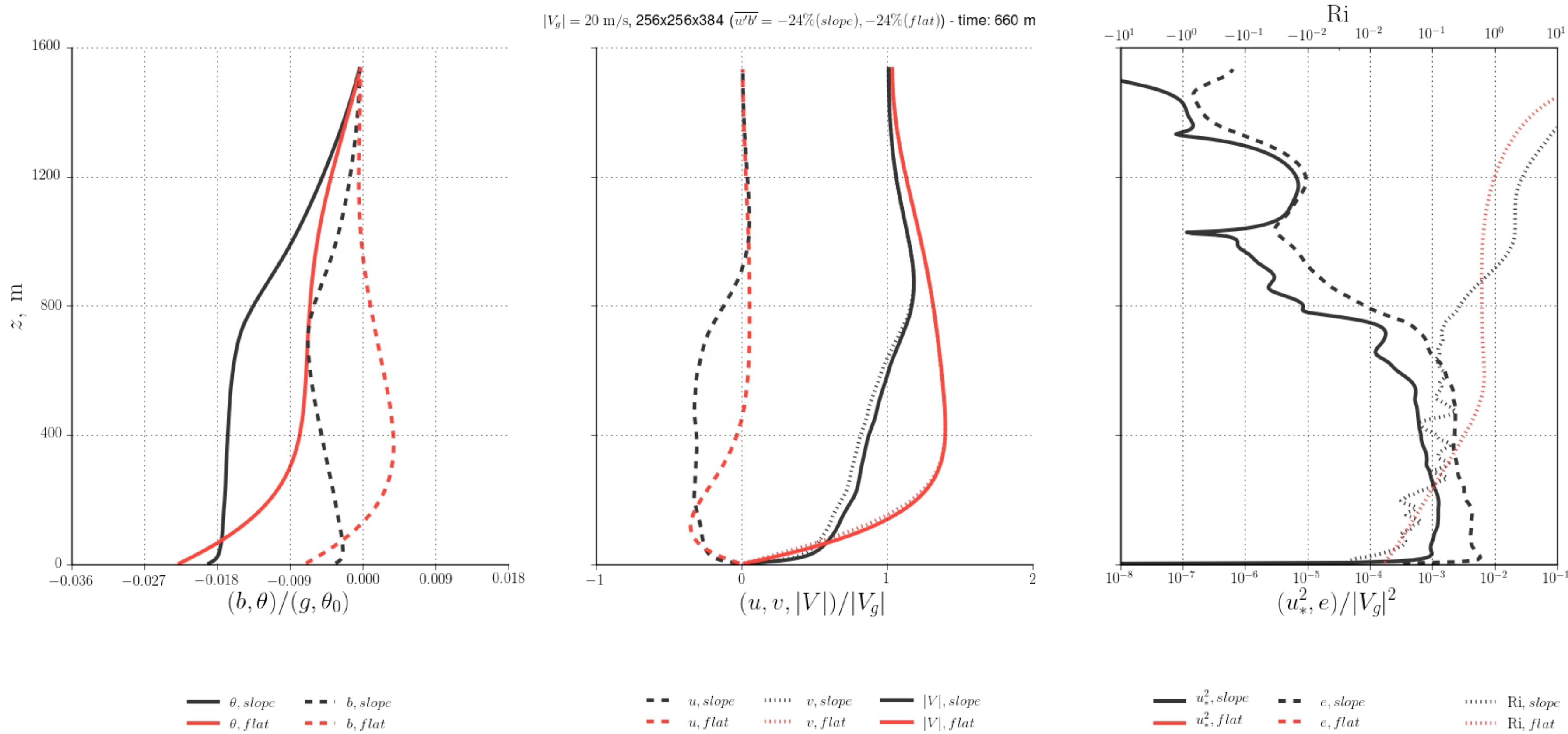

$|V_g| = 20$ m/s, 256x256x384 ($\overline{w'b'} = -24\%(slope), -24\%(flat)$) - time: 660 m
z, m
$(b, \theta)/(g, \theta_0)$
$(u, v, |V|)/|V_g|$
$(u_*^2, e)/|V_g|^2$
Ri
θ, slope
θ, flat
b, slope
b, flat
u, slope
u, flat
v, slope
v, flat
$|V|$, slope
$|V|$, flat
u_*^2, slope
u_*^2, flat
e, slope
e, flat
Ri, slope
Ri, flat

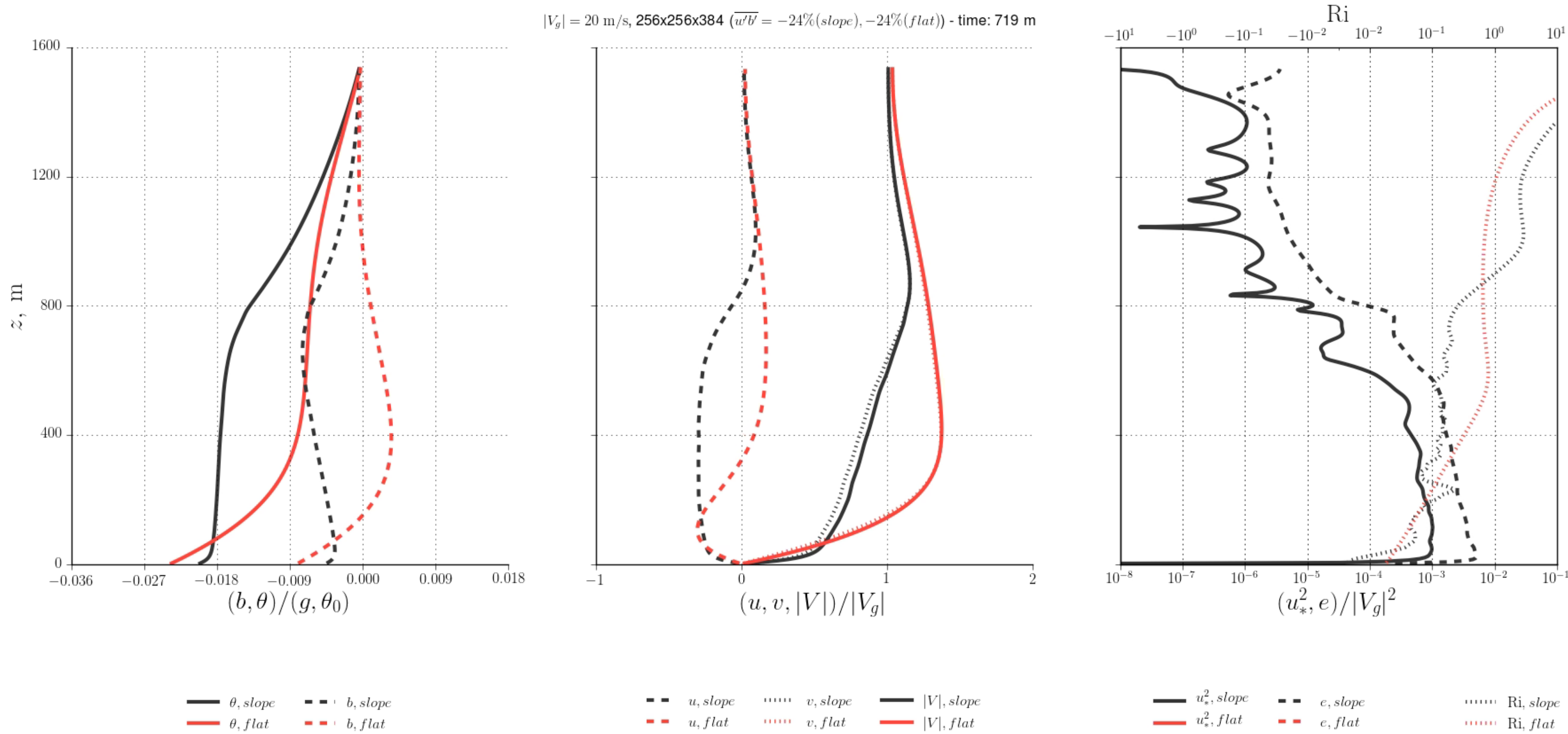

$|V_g| = 20$ m/s, 256x256x384 ($\overline{w'b'} = -24\%(slope), -24\%(flat)$) - time: 719 m
z, m
$(b, \theta)/(g, \theta_0)$
$(u, v, |V|)/|V_g|$
Ri
$(u_*^2, e)/|V_g|^2$
$\theta, slope$
$b, slope$
$\theta, flat$
$b, flat$
$u, slope$
$v, slope$
$|V|, slope$
$u, flat$
$v, flat$
$|V|, flat$
$u_*^2, slope$
$e, slope$
Ri, $slope$
$u_*^2, flat$
$e, flat$
Ri, $flat$

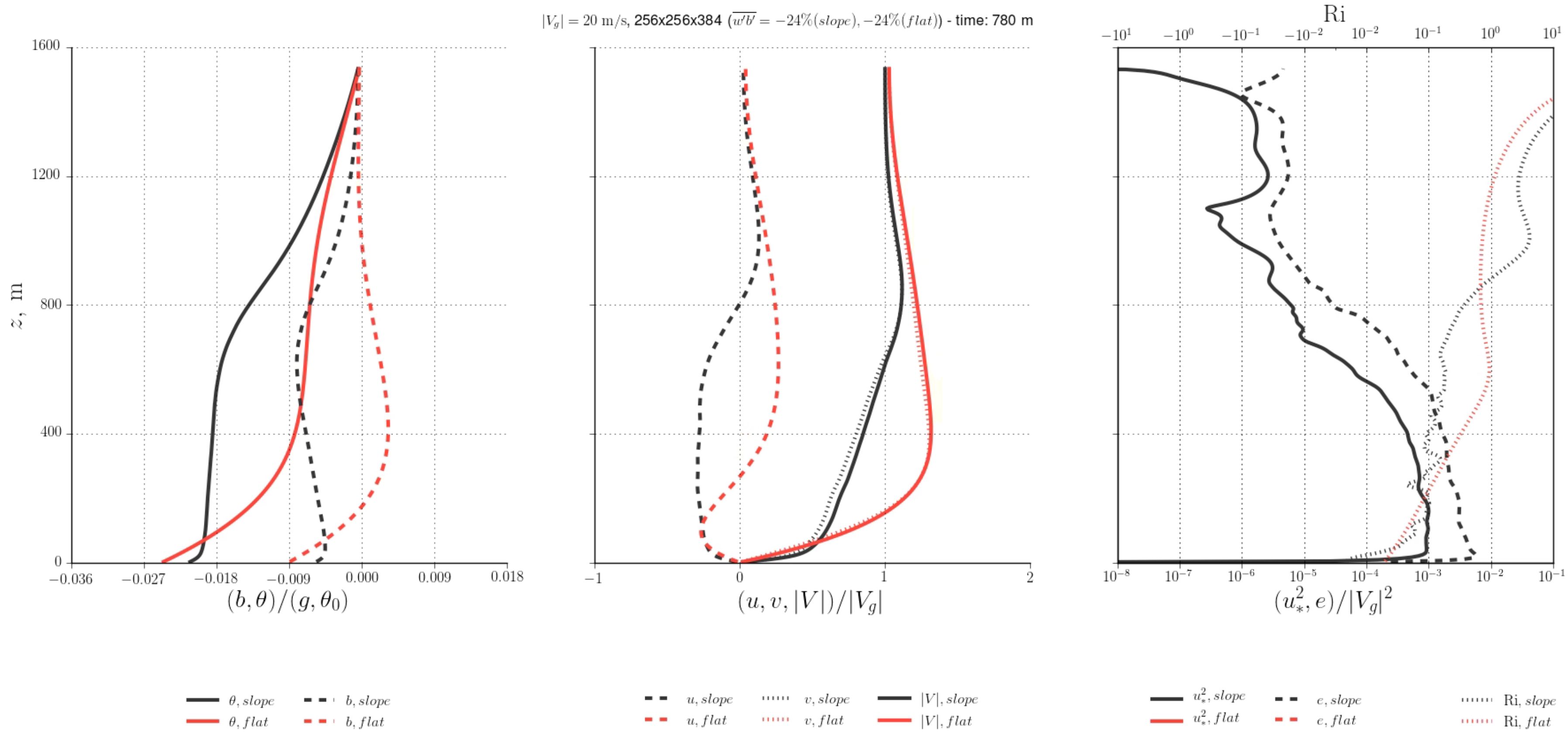

$|V_g| = 20$ m/s, 256x256x384 ($\overline{w'b'} = -24\%(slope), -24\%(flat)$) - time: 780 m
z, m
$(b, \theta)/(g, \theta_0)$
$(u, v, |V|)/|V_g|$
Ri
$(u_*^2, e)/|V_g|^2$
θ, slope
θ, flat
b, slope
b, flat
u, slope
u, flat
v, slope
v, flat
$|V|$, slope
$|V|$, flat
u_*^2, slope
u_*^2, flat
e, slope
e, flat
Ri, slope
Ri, flat

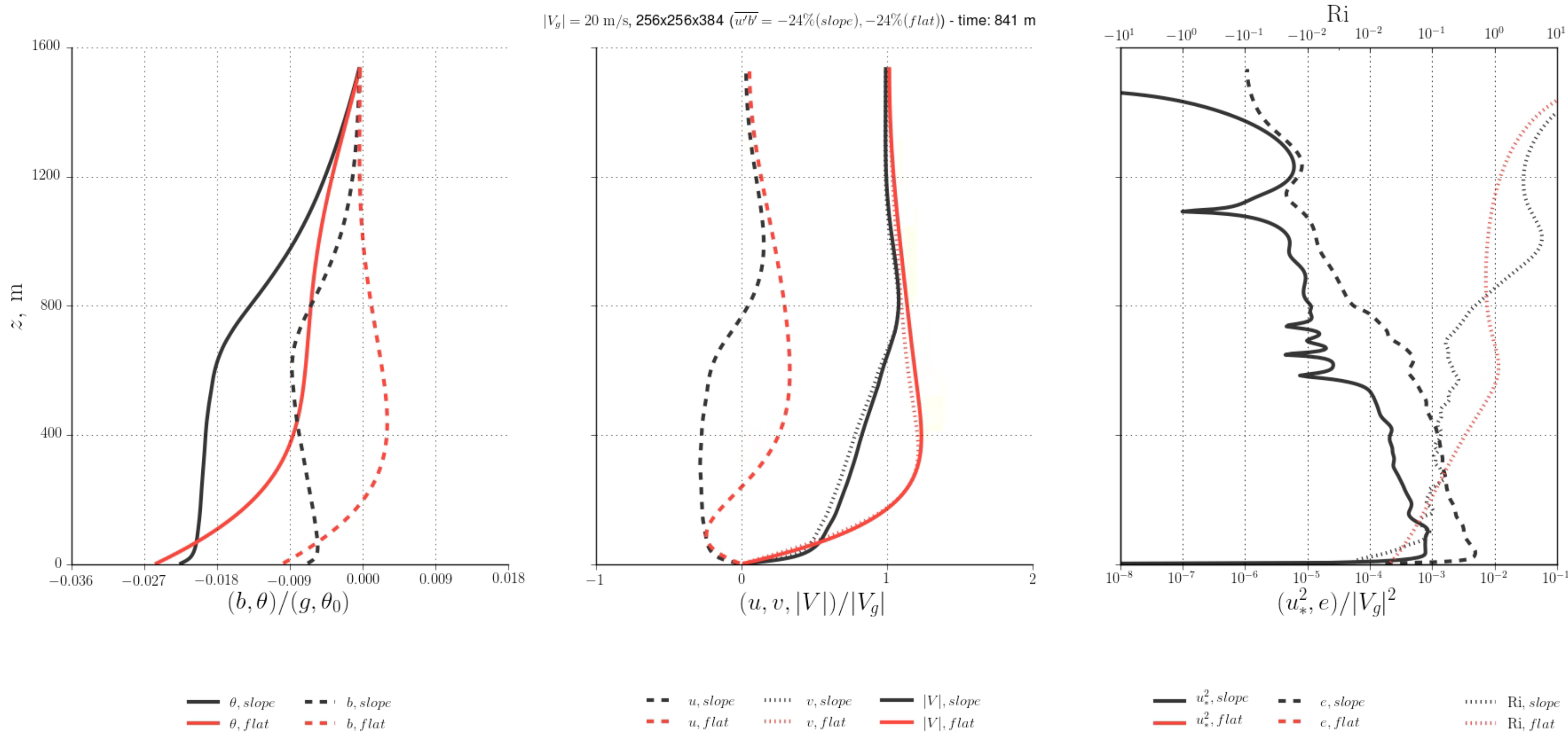
$|V_g| = 20$ m/s, 256x256x384 ($\overline{w'b'} = -24\%(slope), -24\%(flat)$) - time: 841 m
z, m
$(b,\theta)/(g,\theta_0)$
$(u, v, |V|)/|V_g|$
$(u_*^2, e)/|V_g|^2$
Ri
θ, slope
θ, flat
b, slope
b, flat
u, slope
u, flat
v, slope
v, flat
$|V|$, slope
$|V|$, flat
u_*^2, slope
u_*^2, flat
e, slope
e, flat
Ri, slope
Ri, flat

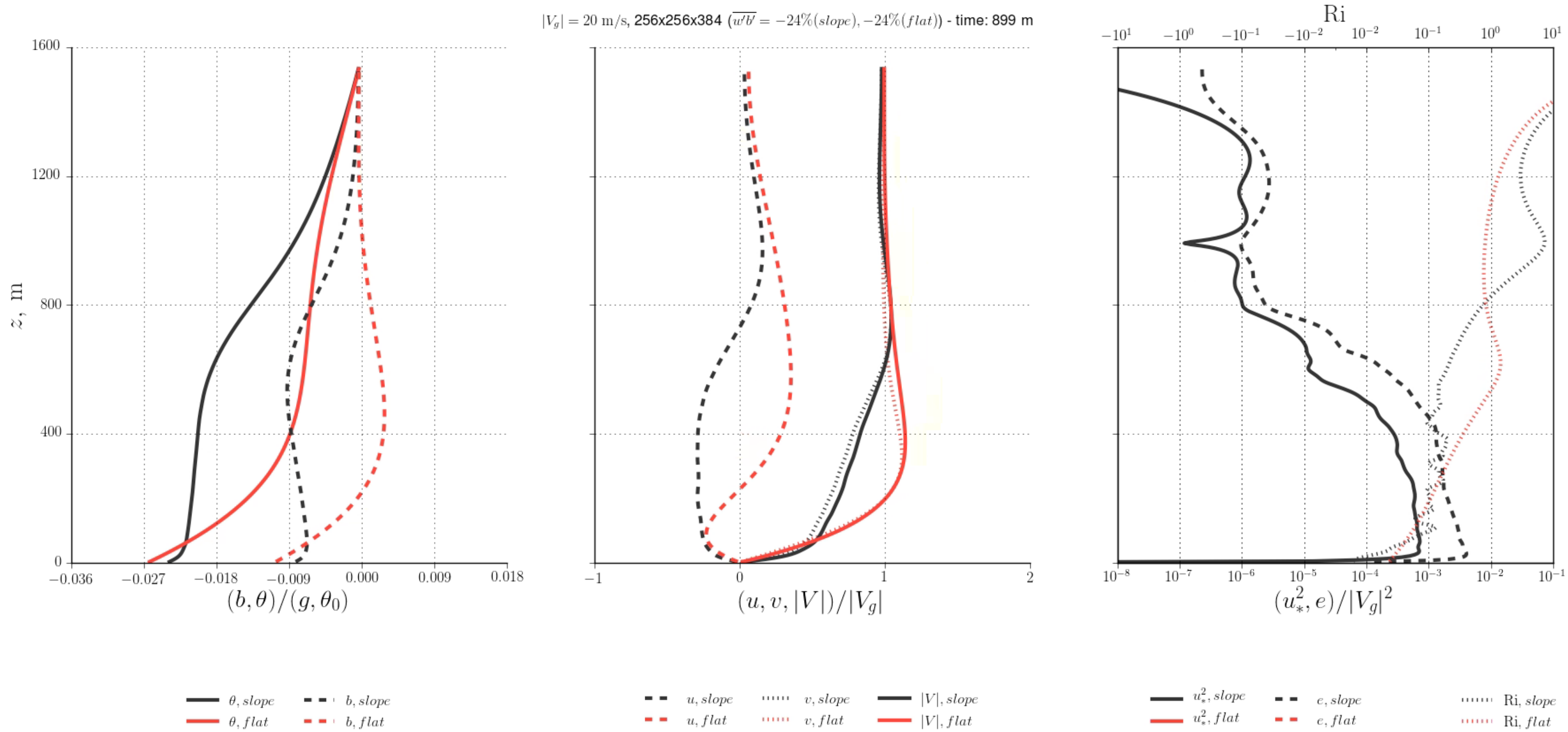

$|V_g| = 20$ m/s, 256x256x384 ($\overline{w'b'} = -24\%(slope), -24\%(flat)$) - time: 899 m
z, m
$(b,\theta)/(g,\theta_0)$
$(u, v, |V|)/|V_g|$
Ri
$(u_*^2, e)/|V_g|^2$
θ, slope
θ, flat
b, slope
b, flat
u, slope
u, flat
v, slope
v, flat
$|V|$, slope
$|V|$, flat
u_*^2, slope
u_*^2, flat
e, slope
e, flat
Ri, slope
Ri, flat

No external geostrophic forcing is needed for LLJ on a slope!

Setup: $\alpha = 0.18^{o}$, $V_g = 0$, $b_{sd} = 0.1\ \mathrm{m\ s^{-2}}$, $b_{sn} = 0$, $N = 2\times10^{-2}\ \mathrm{s^{-1}}$

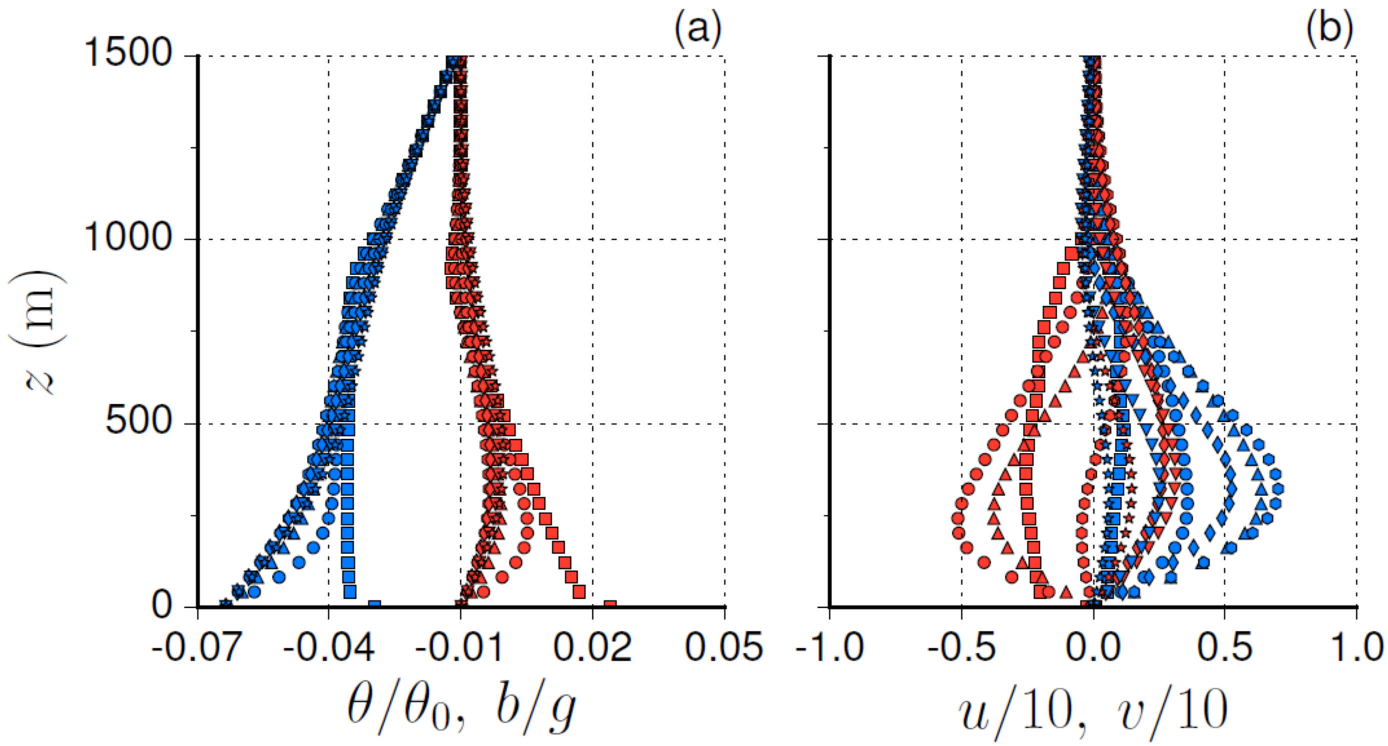

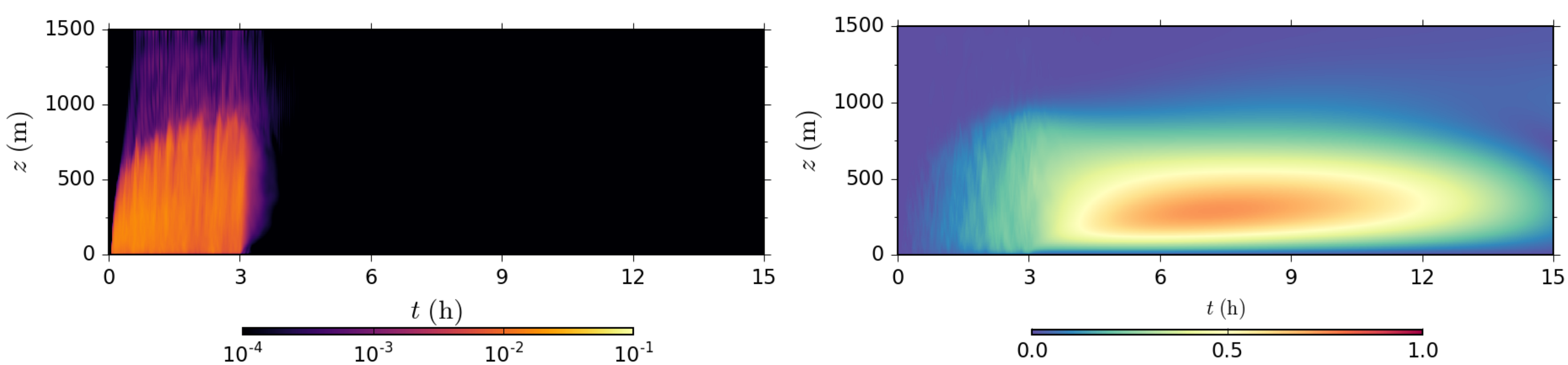

Conclusions

- **Shallow slope affects the LLJ structure and evolution in multiple ways**
- **Along-slope advection of environmental potential temperature can turn a quiet night into a turbulent one, leading to drastic changes in the LLJ properties**
- **Over a slope, a pronounced nighttime LLJ can develop in the absence of external geostrophic forcing**
- **LLJ evolution over a slope depends on the type of surface forcing (buoyancy versus buoyancy flux) much stronger than evolution of the flat-terrain LLJ**
- **Daytime flow preconditioning plays especially important role in LLJ over a slope**

Support from NSF (AGS-1359698) is gratefully acknowledged!

Observed nocturnal LLJ over Great Plains

October 24, 2012, northern Oklahoma

Wind speed from Doppler lidar scans

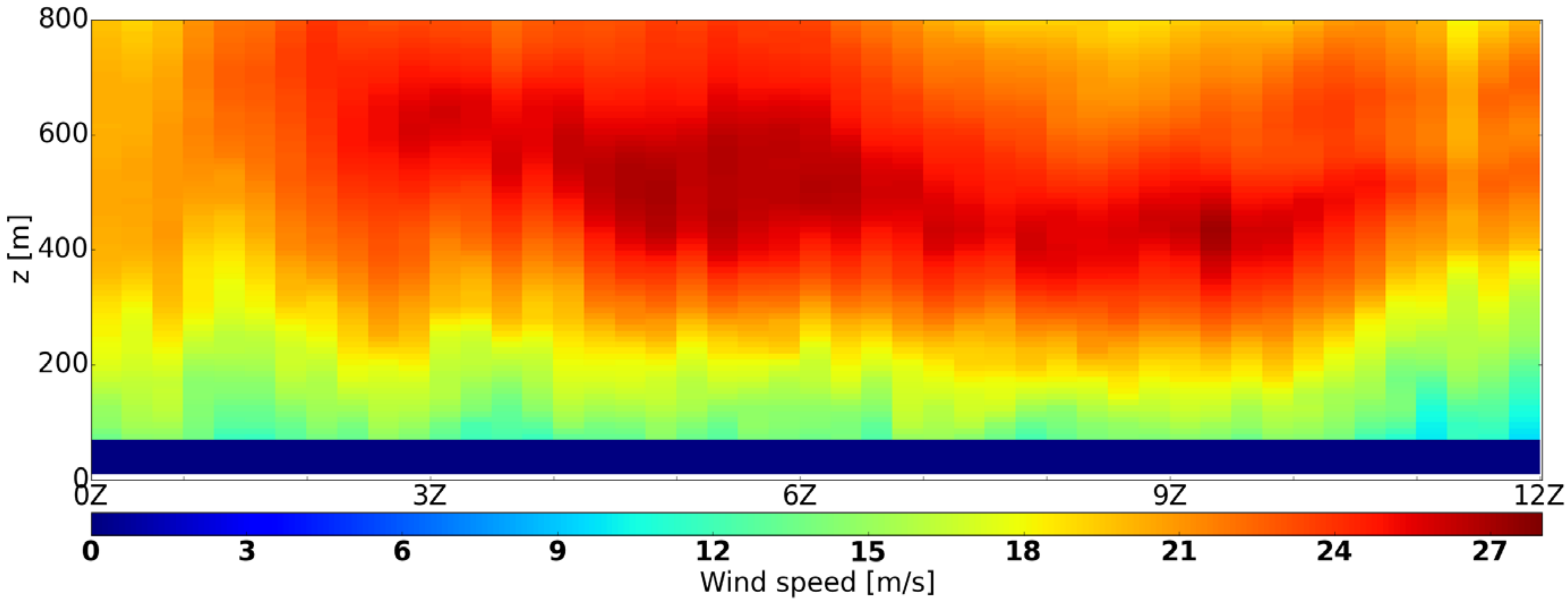

Scaled governing equations

Scales: $V = \left|V_g\right|$ velocity; H (boundary-layer depth ~ domain height) length;

HV^{-1} time; $V^2 H^{-1}$ buoyancy; V^2 pressure.

Normalized governing equations:

$$\frac{\partial u_\mathrm{n}}{\partial t_\mathrm{n}} + u_\mathrm{n}\frac{\partial u_\mathrm{n}}{\partial x_\mathrm{n}} + v_\mathrm{n}\frac{\partial u_\mathrm{n}}{\partial y_\mathrm{n}} + w_\mathrm{n}\frac{\partial u_\mathrm{n}}{\partial z_\mathrm{n}} = -\frac{\partial \pi_\mathrm{n}}{\partial x_\mathrm{n}} + \mathrm{Ro}^{-1}(v_\mathrm{n} - 1) - b_\mathrm{n}\sin\alpha + \mathrm{Re}^{-1}\left(\frac{\partial^2 u_\mathrm{n}}{\partial x_\mathrm{n}{}^2} + \frac{\partial^2 u_\mathrm{n}}{\partial y_\mathrm{n}{}^2} + \frac{\partial^2 u_\mathrm{n}}{\partial z_\mathrm{n}{}^2}\right), \quad (6)$$

$$\frac{\partial v_\mathrm{n}}{\partial t_\mathrm{n}} + u_\mathrm{n}\frac{\partial v_\mathrm{n}}{\partial x_\mathrm{n}} + v_\mathrm{n}\frac{\partial v_\mathrm{n}}{\partial y} + w_\mathrm{n}\frac{\partial v_\mathrm{n}}{\partial z_\mathrm{n}} = -\frac{\partial \pi_\mathrm{n}}{\partial y_\mathrm{n}} - \mathrm{Ro}^{-1}u_\mathrm{n} + \mathrm{Re}^{-1}\left(\frac{\partial^2 v_\mathrm{n}}{\partial x_\mathrm{n}{}^2} + \frac{\partial^2 v_\mathrm{n}}{\partial y_\mathrm{n}{}^2} + \frac{\partial^2 v_\mathrm{n}}{\partial z_\mathrm{n}{}^2}\right), \quad (7)$$

$$\frac{\partial w_\mathrm{n}}{\partial t_\mathrm{n}} + u_\mathrm{n}\frac{\partial w_\mathrm{n}}{\partial x_\mathrm{n}} + v_\mathrm{n}\frac{\partial w_\mathrm{n}}{\partial y_\mathrm{n}} + w_\mathrm{n}\frac{\partial w_\mathrm{n}}{\partial z_\mathrm{n}} = -\frac{\partial \pi_\mathrm{n}}{\partial z_\mathrm{n}} + b_\mathrm{n}\cos\alpha + \mathrm{Re}^{-1}\left(\frac{\partial^2 w_\mathrm{n}}{\partial x_\mathrm{n}{}^2} + \frac{\partial^2 w_\mathrm{n}}{\partial y_\mathrm{n}{}^2} + \frac{\partial^2 w_\mathrm{n}}{\partial z_\mathrm{n}{}^2}\right), \quad (8)$$

$$\frac{\partial b_\mathrm{n}}{\partial t_\mathrm{n}} + u_\mathrm{n}\frac{\partial b_\mathrm{n}}{\partial x_\mathrm{n}} + v_\mathrm{n}\frac{\partial b_\mathrm{n}}{\partial y_\mathrm{n}} + w_\mathrm{n}\frac{\partial b_\mathrm{n}}{\partial z_\mathrm{n}} = \mathrm{BuRo}^{-2}(u_\mathrm{n}\sin\alpha - w_\mathrm{n}\cos\alpha) + \mathrm{Re}^{-1}\left(\frac{\partial^2 b_\mathrm{n}}{\partial x_\mathrm{n}{}^2} + \frac{\partial^2 b_\mathrm{n}}{\partial y_\mathrm{n}{}^2} + \frac{\partial^2 b_\mathrm{n}}{\partial z_\mathrm{n}{}^2}\right), \quad (9)$$

$$\frac{\partial u_\mathrm{n}}{\partial x_\mathrm{n}} + \frac{\partial v_\mathrm{n}}{\partial y_\mathrm{n}} + \frac{\partial w_\mathrm{n}}{\partial z_\mathrm{n}} = 0. \quad (10)$$

Dimensionless parameters of the scaled problem

Rossby number $\mathrm{Ro} = VH^{-1} f^{-1}$ **Reynolds number** $\mathrm{Re} = VH\nu^{-1}$

Burger number $\mathrm{Bu} = N^2 f^{-2}$ b_s-based **Ri number** $\mathrm{Ri} = -b_s H V^{-2}$

N-based **Richardson number** $\mathrm{BuRo}^{-2} = N^2 H^2 V^{-2}$

Atmosphere (ATM):

$V = 10 \text{ m s}^{-1}, \quad H = 10^3 \text{m}, \quad f = 10^{-4} \text{s}^{-1}, \quad N = 10^{-2} \text{s}^{-1}, \quad \nu = 10^{-5} \text{m}^2 \text{s}^{-1}, \quad |b_s| = 0.1 \text{ m s}^{-2};$

$\mathrm{Ro} = 10^2, \ \mathrm{Re} = 10^9, \ \mathrm{Bu} = 10^4, \ |\mathrm{Ri}| = 1$

Length scale range: $\eta \sim (\nu^3 V^{-3} H)^{1/4} \sim 10^{-4} \text{m} \quad \leftrightarrow \quad \sim H = 10^3 \text{m}$

Downscaled laboratory analog of atmospheric flow (LEX):

$V = 0.1 \text{ m s}^{-1}, \quad H = 0.1 \text{ m}, \quad f = 10^{-2} \text{s}^{-1}, \quad N = 1 \text{ s}^{-1}, \quad \nu = 10^{-6} \text{m}^2 \text{s}^{-1}, \quad |b_s| = 0.1 \text{ m s}^{-2};$

$\mathrm{Ro} = 10^2, \ \mathrm{Re} = 10^4, \ \mathrm{Bu} = 10^4, \ |\mathrm{Ri}| = 1$

Length scale range: $\eta \sim (\nu^3 V^{-3} H)^{1/4} \sim 10^{-4} \text{m} \quad \leftrightarrow \quad \sim H = 0.1 \text{ m}$

Viscous atmosphere (VAT):

$V = 10 \text{ m s}^{-1}, \quad H = 10^3 \text{m}, \quad f = 10^{-4} \text{s}^{-1}, \quad N = 10^{-2} \text{s}^{-1}, \quad \nu = 1 \text{ m}^2\text{s}^{-1}, \quad |b_\text{s}| = 0.1 \text{ m s}^{-2};$

$\text{Ro} = 10^2, \ \text{Re} = 10^4, \ \text{Bu} = 10^4, \ |\text{Ri}| = 1$

Length scale range: $\eta \sim (\nu^3 V^{-3} H)^{1/4} \sim 2 \text{ m} \quad \leftrightarrow \quad \sim H = 10^3 \text{m}$

Interpretations:

Integral flow scales in **VAT** are the same as in **ATM**, but the working fluid is way more viscous than the air.

For given α, the equality of flow numbers (Ro, Re, Bu, and Ri) for the small-scale **LEX** flow and for the large-scale **VAT** flow signifies the similarity of these flows in terms of equality of their dimensionless solutions.

VAT simulation may be conceptually interpreted as large-eddy simulation (LES) with constant subgrid eddy diffusivities for momentum and heat/buoyancy.